UNIVERSITÀ DEGLI STUDI DI PADOVA

Dipartimento di Agronomia Alimenti Risorse Naturali e Ambiente

Dipartimento di Scienze Chimiche

University of Szeged

Corso di laurea in Scienze e Tecnologie per l'Ambiente e il Territorio

---

Application of UV, UV/VUV photolysis and ozonation for the decomposition of Sulfamethazine antibiotics in aqueous solution

Relatore: Prof. Valerio Di Marco

Correlatori: Dott. Tünde Alapi

PhD. Luca Farkas

Laureanda: Ilaria Monzini

Matricola n. 1184611

ANNO ACCADEMICO 2019-2020

To my family

Index

1. Abstract

In the present study, the transformation of sulfamethazine (SMT) using UV and UV/VUV photolysis, in presence and absence of dissolved oxygen, ozonation and its combination with UV irradiation have been performed to determine the efficiency of the transformation of the target compound. The transformation of SMT was followed with both UV-Vis spectrophotometry and High Pressure Liquid Chromatography (HPLC) combined with a diode array detector (DAD). Different sulfamethazine concentrations and two mild matrices have been used in order to get to know how they affected the degradation. It was observed that the presence of dissolved oxygen does not increase significantly the effectiveness of the SMT degradation, but it can contribute to enhance the mineralization. Measurements of pH showed no significant effect on the absorbance and transformation rates of SMT. Moreover, the relative contribution of •OH initiated transformation of SMT was studied via addition of terc-buthanol (TBA) as •OH scavenger. The formation of the intermediates during the irradiation time was followed by mass spectrometry with ESI (Electrospray ionization) in negative mode, using SPE as sample pre-treatment method, and four intermediates were detected. The potential degradation pathways of SMT including hydroxylation were proposed. Furthermore, Total Organic Carbon (TOC), Chemical Oxygen Demand (COD), Hydrogen Peroxide (H_2O_2) and NO_3^- concentration were monitored to follow the rate of mineralization during the transformation of SMT. Ecotoxicology tests on *Vibrio fischeri* bacteria were performed in order to investigate the toxicity of the mixture of intermediates formed during the treatment. Based on the Electrical Energy per Order (E_{EO}) values, which define the electrical energy required to decrease the pollutant concentration for one order of magnitude, ozone treatment (0.84 kWh m^{-3} $order^{-1}$) was found to be the most cost-effective method together with the O_3/UV combination (2.31 kWh m^{-3} $order^{-1}$), followed by UV/VUV photolysis (30 kWh m^{-3} $order^{-1}$) and then UV photolysis (52.5 kWh m^{-3} $order^{-1}$).

2. Introduction

2.1 Water pollution focusing on emerging contaminants

Water is one of the essential chemicals for all forms of life on Earth and its quality is highly variable with respect to chemical and microbiological aspects. Due to its important role, water is needed to be preserved. However, the hydrosphere is increasingly polluted as consequence of the high population density and the level of industrialization. This evidence assumes more relevance since the hydrosphere covers about 73% of the Earth's surface, but only about 0.65% of the water total mass can be directly utilized by humans. In recent years, the presence of a group of organic contaminants has been recognized as significant water pollutants. These emerging contaminants (ECs) originate from diverse sources. They are natural or synthetical substances having undesirable effects on humans and the ecosystems. This group includes compounds such as pharmaceutical and personal care products (PPCPs), pesticides, and endocrine disrupting chemicals. The variety of ECs in water has increased over the years, but today's modern analytical techniques have reached so low LOD (detection limit) and LOQ (quantification limit) values, that contaminants can be not only detected but also measured, even at very low concentrations (from ng L^{-1} to µg L^{-1}) (Rodriguez-Narvaez et al., 2017) in various matrices. According to the various applications and properties of water, the treatment technologies are highly diversified. Depending on the source and on the water quality, either mechanical, biological, physical, thermal, chemical processes or their combination may be applied. A typical wastewater treatment plant (WWTP) consists of primary, secondary and tertiary processes (Figure 1). The first are mainly physical treatments to remove precipitable, floating and suspended matter. Secondary treatments are usually realized by biological processes under aerobic and/or anaerobic conditions. The remaining secondary effluent is neutralized and disinfected by chlorine, ozonation or UV radiation during the tertiary procedure before releasing.

The goal of all type of treatment technologies is to attain water quality standards that fulfil government regulations according to emission ordinances.

It has been verified that the natural attenuation and conventional treatment processes are not capable of removing completely the ECs from water (Zeng, 2015). Therefore, they can be transported to surface water and reach groundwater. Because of that, prior to

disinfection, it is recommended to incorporate an additive water treatment technology, which is able to decompose these trace pollutants having low concentration but high risk.

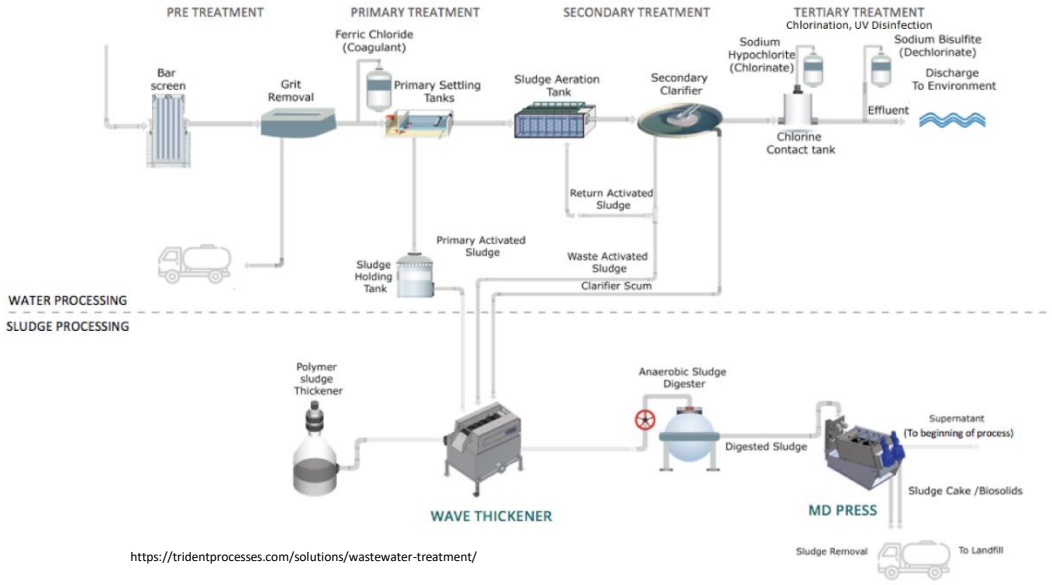

Figure 1. *Scheme of a standard Wastewater Treatment Plant (WWTP)*

The identification of new technologies and the knowledge gaps in relation to the removal of ECs in water is a problem that the scientific community has addressed towards the adoption of better practices to ensure the use of safe drinking water for the community.

2.2 Advanced Oxidation Processes

Application of chemical methods can be an alternative way to enhance water quality.
A special group of these chemical methods is called Advanced Oxidation Processes (AOPs). AOPs are generally based on radical generation, which can be obtained by high energy radiation and/or addition of reactive oxidative components. The most relevant AOPs are summarized in Figure 2.

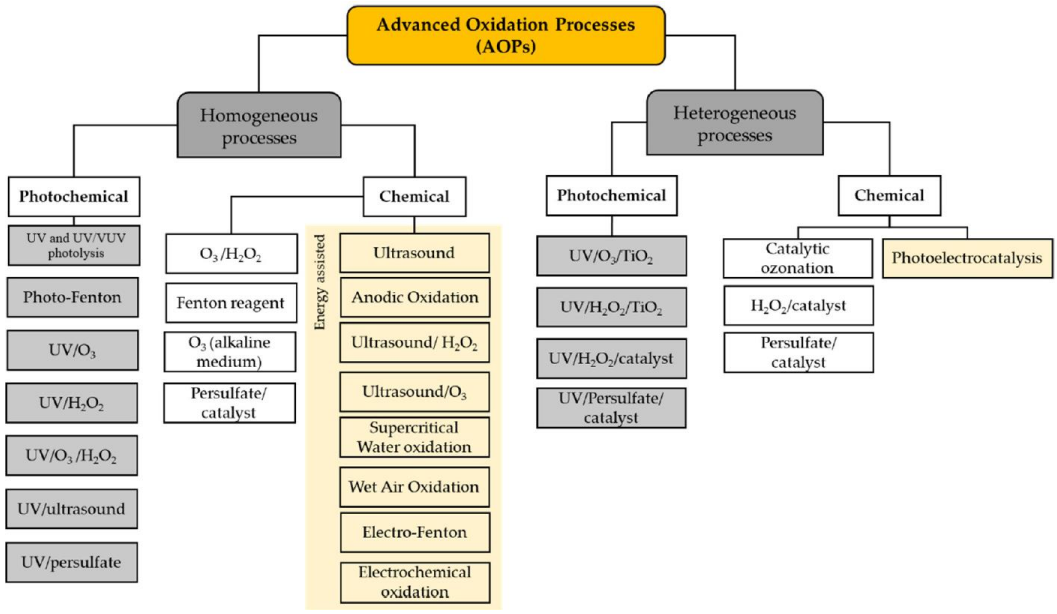

Figure 2. *Family of advanced oxidation technologies (AOPs) for water remediation (redrawn from Amor et al., 2019)*

In particular, photochemical processes were taken into account in this work. They can be classified as follow (Oppenländer, 2003):

1. Photooxidation reactions driven by radiation:
    - Photo-induced oxidations or direct photodegradation, *i.e.* photoionization of molecules induced by adsorption of electromagnetic radiation. This group includes gamma radiolysis, VUV photolysis and UV photolysis. The latter one is generally combined with auxiliary oxidants.
    - Photo-initiated oxidations by H_2O_2, O_3, Cl_2 ($HOCl/OCl^-$), persulfate or other auxiliary oxidants; here the molecules react with a transient and reactive species that is formed from an electronically excited precursor molecule.
    - Photooxygenation reactions; these reactions are often very complex and many competitive reaction pathways may lead to different products (Braun et al., 1991). Many compounds are used as photosensitizers to produce singlet molecular oxygen in solution.
2. Photocatalytic reactions, that are divided in heterogeneous and homogeneous processes and can be operated by two different processes:
    - Photogenerated catalysis: the catalyst is produced by a specified photoreaction involving a precursor molecule, and it reacts with a substrate to form specific products. After that it is fully regenerated.
    - Catalysed photolysis: either the catalyst, or the substrate molecule, or both, are excited by photon absorption during the whole catalytic step.

In some cases, a combination of methods can result in an enhanced efficiency. This is particularly important if the aim is not only the transformation of the organic pollutant but also its complete oxidation: oxidation of organic carbon atoms to carbon dioxide or carbonate species (CO_2, H_2CO_3, HCO_3^-, CO_3^{2-}), hydrogen atoms and heteroatoms (X) conversion into water and corresponding mineral acids (HX), as shown in the reaction below (Oppenländer, 2003):

$C_nH_mX_z \xrightarrow{hv, O_2} nCO_2 + (m - z)/2H_2O + zHX$

As that was mentioned before, AOPs are generally based on radical generation. The most important radical for the transformation and mineralization of organic and inorganic target substances is hydroxyl (•OH) which is the most reactive oxidizing agent in water treatment as it has a very high reduction potential (Table 1).

Table 1. *Reduction potential of common species (Parsons, 2004)*

Species	Reduction potential (V)
Fluorine	3.03
Hydroxyl radical	*2.80*
Oxygen (atomic)	2.42
Ozone	*2.07*
Hydrogen peroxide	1.78
Perhydroxyl radical	1.70
Permanganate	1.68
Hypobromous acid	1.59
Chlorine dioxide	1.57
Hypochlorous acid	1.49
Chlorine	1.36

•OH is a short-lived, non-selective reagent and it is easy to produce. It has electrophilic properties and its reactions with appropriate substrate molecules are kinetically controlled usually exhibiting high second order rate constants between 10^8 and 10^{10} $M^{-1}s^{-1}$. The properties of this radical are resumed in Figure 3.

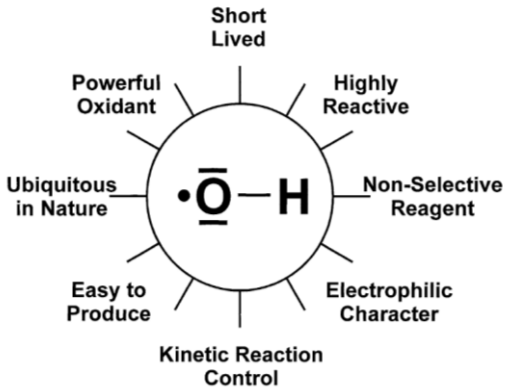

Figure 3. *Some characteristic features of the hydroxyl radical (Oppenländer, 2003)*

•OH is able to attack organic pollutants through various pathways. The most important ones are: addition to aromatic ring or unsaturated carbon-carbon bound, hydrogen abstraction and electron transfer. Finally, radicals can disappear from the system via recombination with other radicals (System SE, 1994). The reaction between •OH and organic substances produces carbon-centred radicals (R–C•–R'). In the presence of O_2, these carbon-centred radicals immediately transform to peroxyl (ROO•), which has a great importance in the subsequent transformation of organic target substances, leading eventually to mineralization (Deng et al., 2015).

•OH can be generated through various ways. The most important ones are the followings (Deng et al., 2015):

1. Ozone based methods are often used as pre- and post- treatment methods and for disinfection:
   - OH^-initiated decomposition of O_3 in aqueous solution (Andreozzi et al., 1999).

     $OH^- + O_3 \rightarrow O_2 + HO_2^-$

     $HO_2^- + H^+ \rightarrow H_2O_2$

     $HO_2^- + O_3 \rightarrow HO_2\bullet + O_3^{\bullet -}$

     $HO_2\bullet \leftrightarrow H^+ + O_2^{\bullet -}$

     $O_2^{\bullet -} + O_3 \rightarrow O_2 + O_3^{\bullet -}$

     $O_3^{\bullet -} + H^+ \rightarrow HO_3\bullet$

     $HO_3\bullet \rightarrow \bullet OH + O_2$

     $\bullet OH + O_3 \rightarrow HO_2\bullet + O_2$
   - Addition of H_2O_2. The method based on the application of a mixture of O_3 and H_2O_2 is called peroxon method (Cuerda-Correa et al., 2019).

     $H_2O_2 \rightarrow HO_2^- + H^+$

     $HO_2^- + O_3 \rightarrow HO_2\bullet + O_3^{\bullet -}$. Followed by typical O_3 decomposition reactions.
2. Radiation based methods:
   - Direct photolysis of water when λ<200 nm (VUV photolysis).

     $H_2O + h\nu \rightarrow \bullet OH + H\bullet$
   - Gamma radiolysis.

     $H_2O + h\nu \rightarrow \bullet OH + H^+ + e^-_{aq}$
   - UV photolysis of hydrogen peroxide, in which several successive and competitive reaction steps can take place (Hernandez et al., 2002).

     $H_2O_2 + h\nu \rightarrow 2\bullet OH$

     $\bullet OH + H_2O_2 \rightarrow H_2O + HO_2\bullet$

$HO_2\bullet + H_2O_2 \rightarrow \bullet OH + H_2O + O_2$

$\bullet OH + HO_2^- \rightarrow HO_2\bullet + OH^-$

$2HO_2\bullet \rightarrow H_2O_2 + O_2$

$\bullet OH + HO_2\bullet \rightarrow H_2O + O_2$

$2\bullet OH \rightarrow H_2O_2$

- UV photolysis of ozone (O_3/UV) (Šojić et al., 2012).

  $O_3 + h\nu \rightarrow O_2 + O^*$

  $O^* + H_2O \rightarrow 2\bullet OH$

  $O_3 + H_2O + h\nu \rightarrow O_2 + H_2O_2$

  $H_2O_2 + h\nu \rightarrow 2\bullet OH$

  $H_2O_2 \leftrightarrow H^+ + \bullet OH$

3. Catalytic processes:

   - Heterogeneous photocatalysis is a widely investigated method. Most often titanium dioxide (TiO_2) is used as photocatalyst. Absorption of light having appropriate wavelength can cause charge separation in the photocatalyst particles. Consequently, radical formation takes place on the surface of TiO_2 particles via charge transfer reactions.

     $TiO_2 + h\nu \rightarrow e^-_{cb} + h\nu^+_{vb}$,

     where "e^-_{cb}" refers to the electrons in conduction band and "$h\nu^+_{vb}$" refers to the positive holes remained in the valence band.

     $h\nu^+_{vb} + OH^-_{(surface)} \rightarrow \bullet OH$

     $h\nu^+_{vb} + H_2O_{(absorbed)} \rightarrow \bullet OH + H^+$

     $e^-_{cb} + O_2 \rightarrow O_2^{\bullet -}$

   - Fenton reaction can be used to treat wastewater in special cases via combination of Fe^{2+} and H_2O_2 addition. Fenton reaction is a multistep chain reaction.

     $Fe^{2+} + H_2O_2 \rightarrow Fe^{3+} + \bullet OH + OH^-$

     $\bullet OH + H_2O_2 \rightarrow HO_2\bullet + H_2O$

     $Fe^{3+} + HO_2\bullet \rightarrow Fe^{2+} + H^+ + O_2^-$

     $Fe^{2+} + HO_2\bullet \rightarrow Fe^{3+} + HO_2^-$

     $Fe^{2+} + \bullet OH \rightarrow Fe^{3+} + OH^-$

   - Photo-Fenton reaction, which consists in a combination of photolysis with Fenton reaction (Oturan et al., 2014).

     $Fe^{3+} + H_2O + h\nu \rightarrow Fe^{2+} + \bullet OH + H^+$

In addition to those mentioned here, there are many other methods. Each method has limitations, advantages and disadvantages. The efficiency and applicability of each method is greatly influenced by the properties of the target compound and the components of the matrix. Various mechanisms simultaneously may occur to remove target pollutants during an AOP treatment. The contribution of the non-radical oxidative mechanisms in the contaminant removal may be dominant or insignificant, depending on the AOP type and reaction conditions.

2.2.1 UV and UV/VUV radiation in photochemistry

In photochemistry, the generally usable wavelengths lie between 170 and 1000 nm, because electronically excited state M* of organic or inorganic molecules M are usually generated by photoexcitation within this wavelength range (Oppenländer, 2003).
The photochemically active region of the electromagnetic spectrum can be divided into five sub bands: the vacuum-UV or VUV (100-200 nm), UV-C (200-280 nm), UV-B (280-315 nm), UV-A (315-400 nm) and VIS (400-780 nm) (Figure 4).

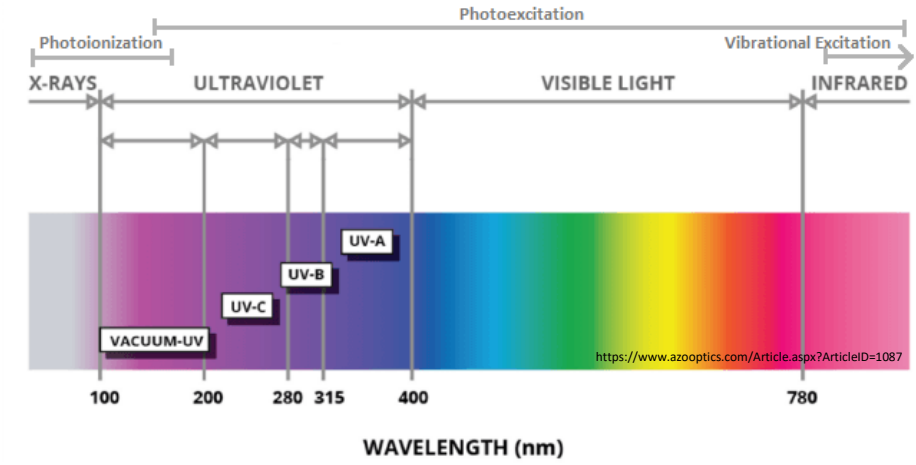

Figure 4. *The electromagnetic spectrum*

The combination of UV/VUV photolysis is an effective advanced oxidation process, with an outstanding efficiency of the degradation of many organic pollutants (Alapi et al., 2007; Náfrádi et al., 2020).

2.2.1.1 VUV photolysis of aqueous solutions

VUV light has enough energy to break chemical bound in almost each organic and inorganic substances. In the gas phase absorption of VUV light by molecular oxygen generates oxygen atoms and eventually ozone.

VUV photolysis is mainly used and investigated for the elimination and mineralization of various pollutants in aqueous solutions. Organic and inorganic molecules or ions have relatively high absorption coefficients in this region. However, the VUV light in aqueous solutions is absorbed almost exclusively by water where its concentration (55.5 mol L^{-1}) substantially exceeds that of the dissolved substances (Parsons, 2004).

In VUV irradiated aqueous solution the absorption of photons causes thus the homolysis of water and formation of •OH and H• (Figure 5):

$H_2O + h\nu$ (<190 nm) → H• + •OH

The quantum yield depends on the wavelength, its value being 0.33 at 185 nm and 0.42 at 172 nm. Another possibility is the photochemical ionization of water molecules, with a much lower quantum yield (0.045) than homolysis (Figure 5):

$H_2O + h\nu$ (<200 nm) → $[e^-_{aq}, H_2O^+] + H_2O \rightarrow e^-_{aq} + \bullet OH + H_3O^+$

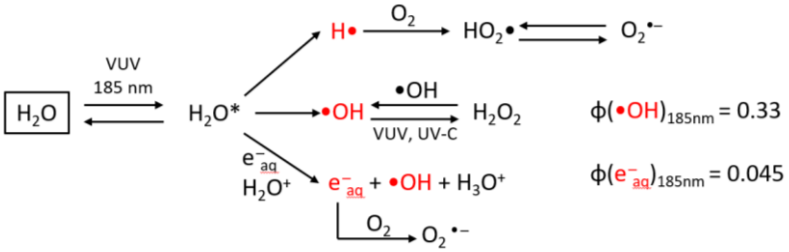

Figure 5. *Reactive species generated by the interaction between VUV radiation and water at 185 nm (redrawn from Opperländer, 2003, p. 192, Figure 7.3)*

As a result of the VUV irradiation of water, the primary formed radicals are H• and •OH. Since e^-_{aq} are present in very low concentrations, their reactions are generally not taken into consideration.

The primary radicals are presumably formed in a solvent cage (Thomsen et al., 1999). Water molecules act as "cage" and prevent the dissociation products (H• and •OH) from breaking through the solvation shell. As a consequence, the recombination of primary radicals such as H• and •OH is highly favoured (László, 2001). Transformation of organic substances is initiated by the H• and •OH, which escape from the "cage".

The dissolved O_2 influences strongly the radical sets. The addition of O_2 to H• results in the production of the less reactive HO_2• radical:

$H• + O_2 \rightarrow HO_2•$ $k = 2.1\times10^{10}$ L mol^{-1} s^{-1} (Buxton et al., 1988)

$HO_2• + H_2O \leftrightarrow H_3O^+ + O_2^{•-}$ pKa = 4.8 (Bielski et al., 1985)

Beside the self-recombination of •OH, the recombination and disproportionation reactions of the radicals generated during the VUV photolysis of aqueous solutions may lead to H_2O_2 production. The main way is most probably the recombination reaction of $HO_2•/O_2^{•-}$:

$O_2^{•-} + HO_2• + H_2O \rightarrow O_2 + H_2O_2 + HO^-$ $k = 9.7\times10^7$ L mol^{-1} s^{-1} (Buxton et al., 1988)

The effectiveness of the process is also determined by the appropriate selection of the lamp type. Two VUV light source are usually used in water treatment: low-pressure mercury vapour lamp (LPM lamp) and Xe excimer lamp.

LPM lamp is made of quartz which contains mercury vapour and an inert gas, mostly argon, with a defined pressure. Mercury atoms (Hg) in the gas phase are electronically excited by an electrical discharge between two electrodes. The electronically excited Hg deactivate to their ground state by emission of radiation according to the energy level diagram (Murov, 1973), generating an intensive radiating arc within the quartz envelope (Opperländer, 2003). The geometry of LPM lamps is mostly tubular and different electrical inputs can be applied. These lamps emit mainly (85-90%) at 253.7 nm and about 7-10% at 184.9 nm (Parsons, 2004) (usually referred to as 254 nm and 185 nm radiation respectively in the technical literature). LPM lamps are also temperature dependent. In order to have high performances, it is necessary to maintain operative temperatures up to 40°C.

In the last years, incoherent excimer lamps have been developed. They exhibit a very long lifetime (in the range of several thousand hours) and extraordinary freedom with respect to the geometric design. Moreover, quasi-monochromatic radiation within a wide UV and VUV spectral region is emitted by simple variation of the gas mixture. The working mechanism of the excimer lamps is based on the formation of short-lived electronically *exc*ited dim*ers* (excimers) containing at least one noble gas. Under suitable condition of the plasma, the excimers decay within nanoseconds with emission of radiation. The commercially available excimer lamp which emits VUV light is based on Xe. Xe-excimer lamp is a 'quasi-monochromatic' light source, which emits VUV light at 172 nm, with full width at half maximum of 14 nm (Eliasson et al., 1988). Generally, the VUV photon flux of Xe-excimer lamp highly exceeds that of LPM lamp. Another important difference is the depth of penetration in water: 185 nm VUV light can penetrate 10 mm, while 172 nm VUV light can penetrate only 0.04 mm (Oppenländer, 2007).

2.2.1.2 UV photolysis of aqueous solutions of organic substances

Application of UV photolysis alone is not an Advanced Oxidation Process. Opposite to the VUV photolysis, where water is the main absorbent, in UV irradiated solutions only the dissolved organic or inorganic substance absorbs the light. Although in some cases in which UV light is capable of exciting and consequently ionizing organic molecules, UV photolysis is primarily used for disinfection.

The efficiency of UV photolysis of organic and inorganic substances depends on the molar absorbance of the substance at the given wavelength and the quantum yield.

When the organic molecules absorb UV light, an electronically excited state RX* is generated. RX* is highly energetic and can either deactivate to the ground state of the molecule through physical processes (such as fluorescence, phosphorescence, or non-radiative deactivation) or undergo "dark" (thermal) chemical reactions (Parsons, 2004). The most common chemical reaction pathways followed by the excited state are summarised in the following set of equations (Parsons, 2004):

$$RX + h\nu \rightarrow RX^* \quad (1)$$

$$RX^* \rightarrow (R^{\bullet}\ldots{}^{\bullet}X)_{cage} \rightarrow R^{\bullet} + {}^{\bullet}X \quad (2)$$

$$(R^{\bullet}\ldots{}^{\bullet}X)_{cage} \rightarrow RX \quad (3)$$

$$RX^* \rightarrow (R^{+}\ldots X^{-})_{cage} \rightarrow R^{+} + X^{-} \quad (4)$$

$$RX^* + O_2 \rightarrow RX^{\bullet+} + O_2^{\bullet-} \quad (5)$$

$$RX^* + {}^3O_2 \rightarrow RX + {}^1O_2 \quad (6)$$

The homolytic bond scission (Equation 2) is the predominant chemical pathway, and it occurs in the solvent cage. Once escaped from the cage, the radicals undergo further oxidation/reduction reactions, depending on their structure.

Organic pollutants may undergo different reaction mechanisms in the presence or in the absence of dissolved O_2, resulting in different end products and affecting the level of mineralisation. Recombination of the primary radicals in the solvent cage (Equation 3) leading to the parent molecule occurs with high probability. In polar solvents, such as water, heterolytic bond scissions (Equation 4) have been observed. Energy and electron-transfer processes (Equations 5 and 6) to oxygen are also possible, but require a relatively long-lived excited state, such as the triplet state. Proton and hydrogen atom transfers from the excited state to surrounding molecules are also possible, but with a much lower probability than the reactions above.

UV photolysis can be used as an effective AOP with a combination of different oxidants (H_2O_2, O_3, Cl_2) for efficient elimination of organic pollutants.

The photolysis of H_2O_2 occurs in a range between 200 and 300 nm, leading to the formation of •OH radicals which can also contribute to the decomposition of H_2O_2 by secondary reactions (Hernandez et al., 2002). The major drawback of this process is the small absorption coefficient of H_2O_2 which is only 18.6 M^{-1} cm^{-1} at 254 nm (Deng et al., 2015), making it necessary to use a rather large concentration of H_2O_2 for an efficient oxidation of organic pollutants (Oturan et al., 2014). Generally, the reaction rate is larger at pH > 10 in which hydrogen peroxide deprotonates with formation of HO_2^-. These species has a significantly higher absorption coefficient than H_2O_2, competing for UV radiation and producing free radicals (HO_2• and •OH). The H_2O_2/UV system is often preferable to ozonation because it is less sensitive to the nature and concentration of the polluting species (Cuerda-Correa et al., 2019).

2.2.2 Ozone based processes

Ozone is a powerful oxidant and has many industrial and consumer applications related to oxidation. Ozonation is useful in disinfection of potable water, in wastewater treatment and in many other applications. Though disinfection of wastewaters is often achieved with chlorine or UV rather than ozone, the growing importance of water reuse and micropollutant removal may render ozone more attractive because of its dual role as disinfectant and oxidant (von Sonntag et al., 2012).

The ozone molecule is moderately stable. It decomposes within several days with the formation of stable O_2. The decay is accelerated drastically in the presence of catalysts, by elevated temperatures and by UV-B/UV-C irradiation. Owing to the instability of the ozone molecule, it can neither be shipped nor stored in gas tanks (Oppenländer, 2003). Therefore, it must be produced on site. O_3 can be generated by photochemical way via VUV photolysis of O_2. A more economical way is the corona discharge or the Siemens method. This is the most common type of ozone generator for most industrial and personal uses. They are typically cost-effective and do not require an oxygen source other than the ambient air to produce ozone concentrations of 3-6%. The reactions taking place in the discharge space are the followings (von Sonntag et al., 2012):

$O_2 + e^- \rightarrow O_2^* + e^-$

$O_2^* \rightarrow 2O(^3P)$

$O(^3P) + O_2 + M \rightarrow O_3^* + M \rightarrow O_3 + M$

M is the collision partner and it can be O_2, O_3, O or N_2.

Solubility of O_3 in water at 0°C is 4.9 ml L^{-1}. The solubility depends on temperature, pressure and on solution pH. Aqueous ozone solutions are also unstable, especially basic solution, because HO^- initiates the decomposition of ozone as shown in Figure 6.

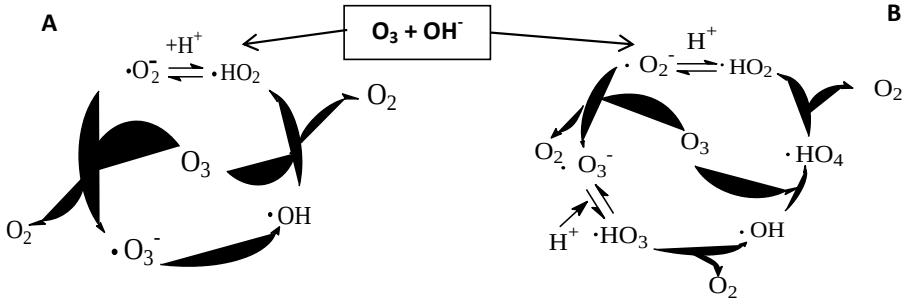

Figure 6. *TFG (A) and SBH (B) models for the HO^- initiated cycle of ozone decomposition (Ragnar et al., 1999)*

Due to the enhanced generation of hydroxyl radicals under such conditions, it is possible to consider ozonation at high pH (>8) (Ikehata et al., 2006).

Ozone is a very selective reaction partner. The rate constant of the reactions between ozone and organic matter varies widely depending on the structure of organic substance, and their values fall in the range 10^{-4}-10^9 M^{-1} s^{-1}. The ozone molecule is an electrophilic reagent that reacts selectively with organic compounds having nucleophilic moieties such as carbon-carbon double bounds, aromatic rings, and the functional groups bearing sulphur, phosphorus, nitrogen or oxygen atoms to form unstable ozonides.

Beside HO^-initiated transformation, the addition of hydrogen peroxide in ozonation may help to improve the mineralization process efficiency, since the reaction of O_3 with H_2O_2 results in the generation of •OH radicals (Cuerda-Correa et al., 2019). The pollutant dissolved in water is thus susceptible to undergo oxidation through different routes: the direct route (molecular reaction with ozone) or the indirect radical pathway (reaction with the hydroxyl radical). Additionally, ozone may also react directly with hydrogen peroxide and additional hydroxyl and ozonate radicals are generated:

$2H_2O_2 + O_3 \rightarrow 2\bullet OH + O_3^-$

The non-selective and highly reactive •OH can be also produced by the UV-initiated transformation of ozone. The highest absorption band of ozone in aqueous solution is in

the UV region and it covers a range from 200 nm to 300 nm approximately. The photolysis of O_3 (ε_{254nm} = 3000±30 M^{-1} cm^{-1}, $\phi(O_3)$ = 0.48±0.6 (Gurol et al., 1996)) produces •OH that can react with organic compounds, enhancing the transformation and mineralization efficiency. Thus, LPM lamp that emits at 254 nm is an excellent light source to realize UV/O_3 combined method. O_3 molecules produce reactive species, such as •OH and H_2O_2, through direct photolysis (Šojić et al., 2012). The H_2O_2 formed is also transformed to reactive •OH via direct photolysis. While the efficiency of simple ozonation depends strongly on the pH of the solution, the pH dependence is negligible in the case of UV/O_3 combination.

It is possible to couple all the features seen previously in a tertiary H_2O_2/O_3/UV system. The main advantage of this system lies in the fact that the decomposition of ozone is speeded up by the simultaneous reactions that occur among the elements, thus yielding an increased rate of generation of •OH radicals (Cuerda-Correa et al., 2019). However, the high costs of the three elements that constitute the system pose a remarkable disadvantage that limits a broader use of this process. Consequently, the use of this ternary system is usually restricted to the treatment of highly polluted effluents to achieve adequate degradation and mineralization of recalcitrant pollutants.

2.2.3 Possibility of applications in wastewater treatment plants

In order to be functional, it is important to install AOPs in strategic points. Pollutants can be eliminated completely through mineralization or converted to less harmful products. As the partial degradation of organic compounds generally enhance their biodegradability (Alvares et al., 2001), AOPs can be used as pretreatment prior to biological processes. However, this approach may not be appropriate where organic matter is predominantly present because oxidant requirement can be exceedingly high (Ikehata et al., 2006). Thus, it is more feasible to install these processes as tertiary treatment after the biological one, when the wastewater is already partially treated but recalcitrant organic contaminants are not sufficiently removed. If the target is drinking water, the addition of preoxidation and/or disinfection steps is also required.

Some conventional water quality parameters can be used to evaluate the effectiveness of the process, such as Total Organic Carbon (TOC) and Chemical Oxygen Demand (COD). However, they do not provide direct information about the identity of degradation

products and the safety of treated water. Other parameters are useful to calculate and compare the effectiveness of different systems regardless of their configurations. The most important one is the Electrical Energy per Order (E_{EO}), which refers to the electrical energy in kilowatt hours (kWh) required to degrade a contaminant by one order of magnitude in a unit volume of water (Parsons, 2004). A lower E_{EO} value leads to lower power costs. Consequently, this value has to be minimised in order to reduce outflows during the project lifetime.

The knowledge of kinetic parameters of the reactions involving organic pollutants is also an important factor to select and optimise the appropriate treatment technology. However, they are not easy to characterise, because photochemical reaction kinetics are affected by water constituents (such as absorbers, photosensitizers and suspended solids, etc.), pH, ionic strength, concentration of dissolved oxygen and temperature. Furthermore, the costs of materials and equipment, as well as energy requirements and efficiency must be considered when assessing the overall performance of AOPs.

2.3 Antibiotics: sources, global consumption, adverse effects

Over the past few years, antibiotics (ABs) have been considered emerging contaminants due to their continuous input and persistence in the aquatic ecosystem, most often at low concentration. ABs are defined as chemical compounds that are synthesized through the secondary metabolism of living organisms, with exceptions for semi- or completely synthetic substances (Thiele-Bruhn, 2003). They inhibit the activity of microorganisms, viruses, and eukaryotic cells for the treatment of multiple types of infectious diseases, both in humans and animals. The use of ABs is widespread, and they have been detected in different matrices. These pollutants are continually discharged into natural environment by a diversity of input sources as shown in Figure 7.

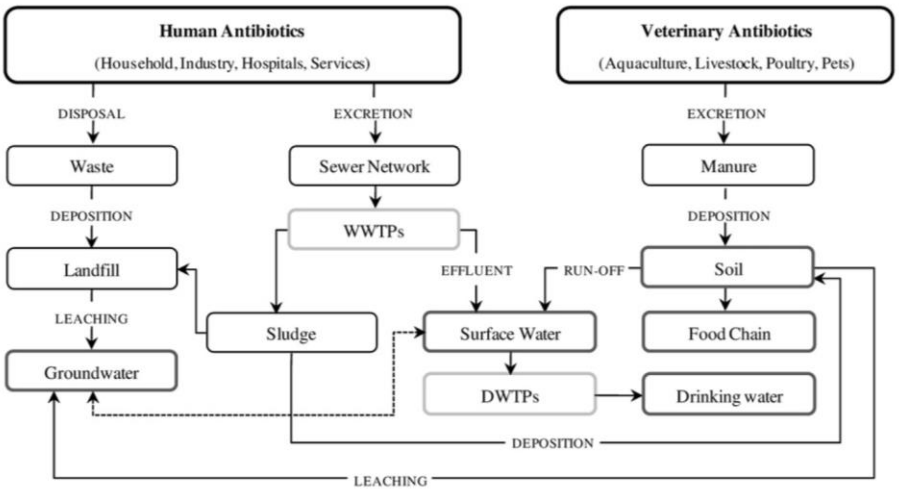

Figure 7. *Sources and principal contamination routes of human and veterinary antibiotics (Homem et al., 2011)*

ABs from human usage are introduced into the environment through excretion (urine and faeces), entering in the sewer network and reaching the wastewater treatment plants. As already mentioned, most of WWTPs and drinking water treatment plants (DWTPs) are not designed to remove recalcitrant pollutants like ABs, which undergo mechanical, chemical and biological processes. Moreover, the sludge produced in WWTPs can still contain contaminants that are transferred in the soil through fertilization.

Another main source of ABs effluence is livestock manure, because animal feed is often supplemented with veterinary antibiotics (VABs) to promote growth and disease prevention. After the administration, AB compounds are absorbed, distributed, metabolized and excreted from the body. Therefore, like other pharmaceuticals, VABs are optimized in their pharmacokinetics in such a way that they do not accumulate in the organism. (Thiele-Bruhn, 2003). Consequently, the excess is excreted as parent compounds without any biotransformation process. Once in the soil, these ABs can transfer into the food chain or spread to the groundwater and the surface water by infiltration and runoff, respectively.

Many countries have already restricted AB use in animal's nutrition. In 2006, the European Union banned the use of AB as growth promoters in animal food and water. Anyway, more restrictions should be implemented as the global consumption of ABs in animals is twice than for humans, rising to four times higher in Unites States in 2012 (Indranil et al., 2020). A study by Van Boeckel et al. (2015) displayed a significant geographic heterogeneity of AB consumption throughout the world (Figure 8). In the upper graphic more homogeneous areas are presented where livestock farming is well established, while a hotspots design is characteristic of developing regions.

The graphic below shows the standard deviations (SDs) of the base parameters of the modelling study. In general, the values of these coefficients discriminate the uncertainty in the model prediction: a decreasing value means a better matching where intensive farming practices are common and food animals are densely populated.

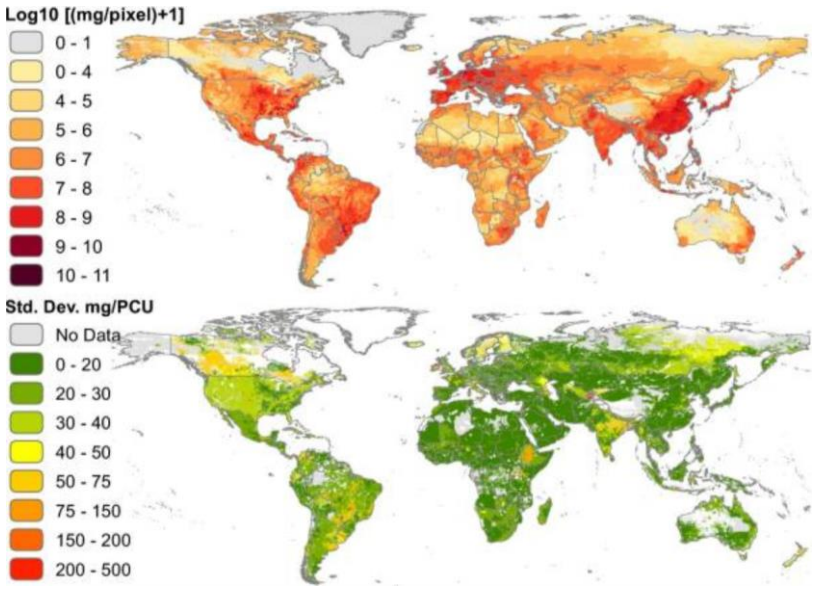

Figure 8. *Global antimicrobial consumption in livestock in milligrams per 10 km^2 pixels (Above) and average SD of estimates of milligrams per population correction unit (PCU) (Bottom)*

However, the meat consumption is growing in the middle- and low-income countries (such as BRICS: Brazil, Russia, India, China, and South Africa). Because of that, recent projections estimate that the worldwide use of VABs will rise by 67% in 20 years: from 63151 tons in 2010 to 105596 tons in 2030 (Van Boeckel et al., 2015). Another reason for the increment of such quantity is imputable to a shift in farming system to large-scale farms, where VABs are used more intensively.

The introduction and persistence of ABs in the environment can produce harmful effects, either in aquatic and terrestrial ecosystems as well as public health risks. Among the adverse effects, such as anomalous physiological developments, reproductive destructions, increase of cancer, endocrine disruption and imbalance of microbial ecosystems; the most relevant is the development of antimicrobial resistance (AMR) in bacteria. This phenomenon is driven by a genetic selection of resistant bacteria, an irreversible effect favoured by low concentrations of the AB and the repeated exposure to it. AMR is accelerated by the overuse of pharmaceuticals. Especially in agriculture, ABs are often used to compensate for insufficient hygiene in stable and for not species appropriate animal husbandry (Thiele-Bruhn, 2003).

A microorganism may have either intrinsic or acquired resistance to an AB (McManus, 1997). Intrinsic resistance is a stable genetic property encoded in the chromosomal DNA and shared by all members of the genus (vertical resistance transfer). Acquired resistance occurs when there is a change in the bacterial DNA so that a new phenotypic trait can be expressed. Bacteria can acquire resistance through a mutation in the host's chromosomal DNA or by acquisition of new DNA that carries information for resistance (horizontal resistance transfer). This latter mechanism acts in three different ways (Gothwal et al., 2014): a) conjugation, bacterial plasmid transfer from one bacterium to another; b) transduction, viral mediated (phage) gene transfer; c) transformation, the uptake of naked DNA via the cell wall and the incorporation of that DNA into the existing genome or plasmids.

The resistance to ABs leads to the reduction of therapeutic potential against human and animal pathogens, compromising the ability to treat common infectious diseases. Moreover, there are evidence that the resistance of bacteria can be transmitted to humans through the environment (Graham et al., 2009), food products (Price et al., 2005) and to agricultural workers by direct contact (Smith et al., 2013).

The European Antimicrobial Resistance Surveillance Network (EARS-Net) provides annual reports about the surveillance of AB resistance in Europe (ECDC, 2019). Recent estimates show that each year, more than 670000 infections occur in the EU/EEA due to bacteria resistant to ABs, and that approximately 33000 people die as a direct consequence of these types of infection. The related cost to the healthcare systems of EU/EEA countries is around 1.1 billion euro.

2.3.1 Sulphonamides

Antibiotics can be classified into different classes with regard to their chemical structure, action mechanism, action spectrum and the route of administration. In Table 2, the most representative ABs are listed with further information on their typical ranges of some physicochemical properties.

Table 2. *Representative pharmaceutical antibiotics and typical ranges of physicochemical properties (Thiele-Bruhn, 2003)*

Class	**Molar mass** g mol^{-1}	**Water solubility** mg l^{-1}	**Partition coefficient** logK_{ow}	**p*K*a**	**Henry's law constant (K_H)** Pa l mol^{-1}
Tetracyclines	444.5–527.6	230–52000	-1.3–0.05	3.3/7.7/9.3	1.7×10^{-23}–4.8×10^{-22}
Chlortetracycline, oxytetracycline, tetracycline					
Sulphonamides	172.2–300.3	7.5–1500	-0.1–1.7	2–3/ 4.5–10.6	1.3×10^{-12}–1.8×10^{-8}
Sulphanilamide, sulfadiazine, sulfadimidine, sulfamethoxine, sulfapyridine, sulfamethoxazole					
Aminoglycosides	332.4–615.6	10–500	-8.1– -0.8	6.9–8.5	8.5×10^{-12}–4.1×10^{-8}
Kanamycin, neomycin, streptomycin					
B-Lactams	334.4–470.3	22–10100	0.9–2.9	2.7	2.5×10^{-19}–1.2×10^{-12}
Penicillins: ampicillin, meropenem, penicillin G; cephalosporins: ceftiofur, cefotiam					
Macrolides	687.9–916.1	0.45–15	1.6–3.1	7.7–8.9	7.8×10^{-36}–2.0×10^{-26}
Erythromycin, oleandomycin, tylosin					
Fluorquinolones	229.5–417.6	3.2–17790	-1.0–1.6	8.6	5.2×10^{-17}–3.2×10^{-8}
Ciprofloxacin, enrofloxacin, flumequin, sarafloxacin, oxolinic acid					
Imidazoles	171.5–315.3	6.3–407	-0.02–3.9	2.4	2.3×10^{-13}–2.7×10^{-10}
Fenbendazole, metronidazole, oxfendazole					
Polypeptides	499.6–1038	Not-completely	-1.0–3.2		Negligible–2.8×10^{-23}
Avermectin, bacitracin, ivermectin, virginiamycin					
Polyethers	670.9–751.0	$2.2\text{x}10^{-6}$–$3.1\text{x}10^{-3}$	5.4–8.5	6.4	2.1×10^{-18}–1.5×10^{-18}
Monensin, salinomycin					
Glycopeptides	1450.7	>1000	Not soluble in octanol	5.0	Negligible
Vancomycin					
Quinoxaline-derivatives **olaquindox**	263.3	1.0×10^{6}	-2.2	10	1.1×10^{-18}

The use of ABs has begun with sulphonamides in 1935. In that year, the German pharmaceutical manufacturer Bayer marketed Prontosil (*Prontosil rubrum*), referring to the molecule of sulfochrysoidine (Kirchhelle, 2018). For this discovery Gerhard Domagk was awarded the Nobel Prize in Medicine in 1939. Prontosil was the first effective drug against Gram-positive infections to use in the medical field. By the end of the decade, other compounds related to sulphonamides were introduced and extended to agriculture. Sulphonamides are synthetic antibiotics composed by a variety of compounds having a common chemical structure: a sulphonamide group and an amino group in the para position of the benzene ring, called "*p*-aminobenzene" core (Figure 9). They can also be named as sulfonamides or sulpha/sulfa drugs.

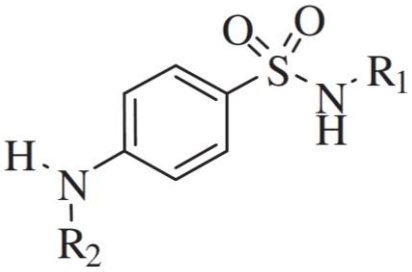

Figure 9. *Common chemical structure of sulphonamides*

Sulphonamides are synthesised through different type of reactions. The most common is the involvement of corresponding aliphatic or aromatic sulfonyl chloride with ammonia or an adequate amine (Tačić et al., 2017).

The obtained products differ for the substitution of the atom on the nitrogen of the sulphonamide group (R1), whereas substitutions on the aromatic amino group (R2) are less frequent. The introduction of various substituents resulted in sulphonamide derivatives with different physicochemical, pharmacokinetic and pharmacodynamic properties. The structures of some important sulphonamides are presented in Figure 10.

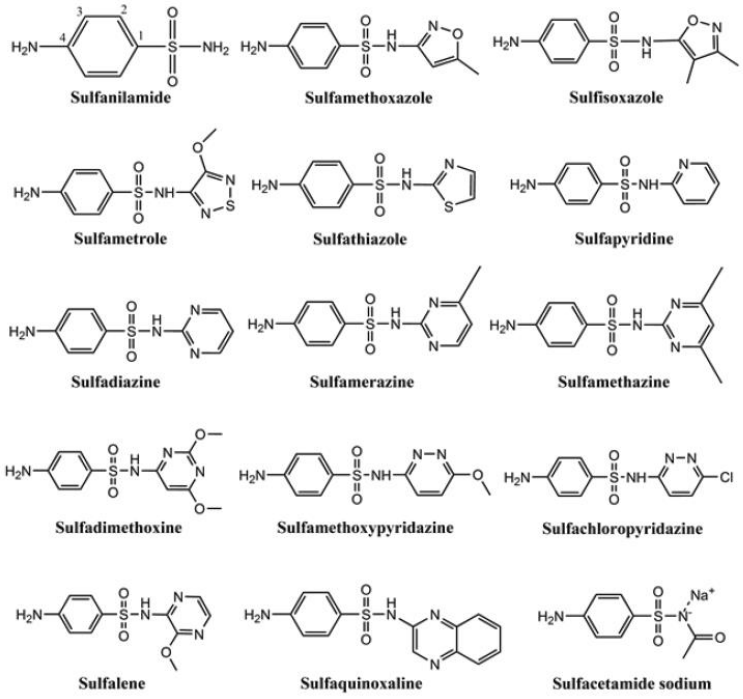

Figure 10. *Structures of several sulphonamide antimicrobial drugs*

In general, as shown in Table 2, sulphonamides are weak acids and form salts in strongly acid or basic solutions (Thiele-Bruhn, 2003). They are non-volatile compounds (K_H), relative soluble in water with low partitioning properties (logK_{ow}). On the other hand, they

are classified as persistent organic pollutants (POPs), due to their resistance to biodegradation (Sági et al., 2015).

The NH_2 group in the para position and the sulphonamide group directly attached to the benzene ring are essential for the antimicrobial activity. Compounds with additional or different substituents lead to the reduction or a complete loss of effectiveness.

Sulphonamides have a broad spectrum of action against Gram-positive and certain Gram-negative bacteria, such as *Escherichia coli*, *Klebsiella*, *Salmonella* and *Enterobacter* species. Other microorganisms can be treated among virus, protozoa (*Toxoplasma gondii*) and fungi (*Pneumocystis carinii*). The effectiveness and the potency of action vary among microorganisms.

The AB action mechanism involves the *p*-aminobenzoic acid (PABA), an essential compound for the synthesis of folic acid which takes part to the bacterial growth and reproduction processes. Sulphonamides basic structure is very similar to the one of PABA (Figure 11a). Thus, they can reversibly inhibit the synthesis of folic acid by replacing PABA in the bound with the dihydropteroate synthase enzyme (DHPS), preventing the DNA and RNA synthesis (Figure 11b). The whole antimicrobial effect is bacteriostatic, rather than bactericidal. Human and animal cells do not synthesize folate so that sulphonamide compounds cannot affect their metabolism.

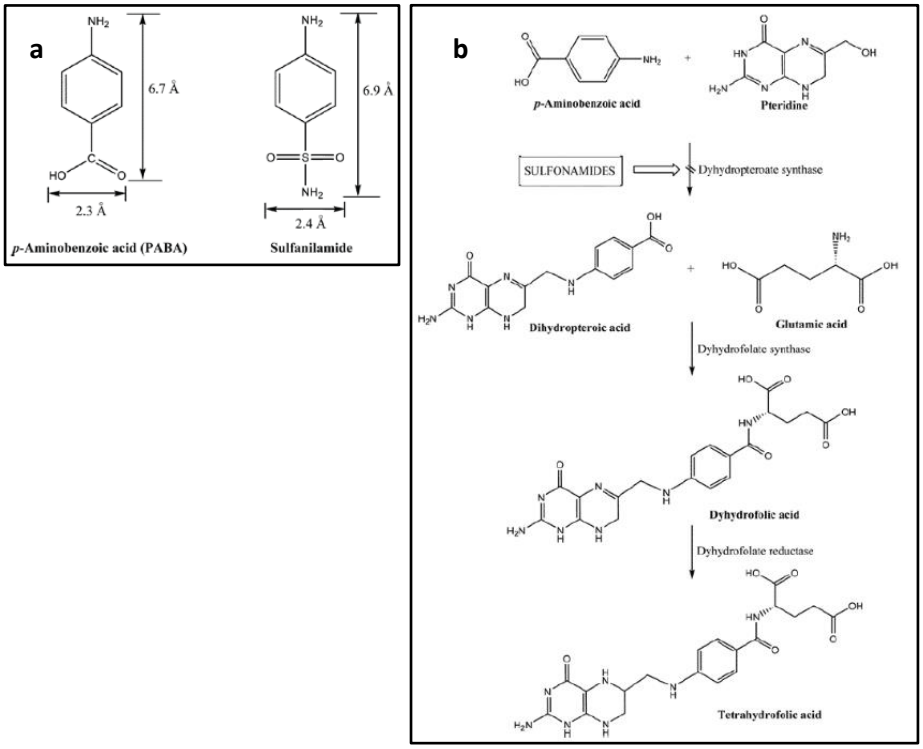

Figure 11. *a) Structure similarity of sulphanilamide and p-aminobenzoic acid (PABA); b) Folic acid synthesis and sulphonamides site of action (Tačić et al., 2017)*

Due to their bacteria inhibition action, sulphonamides are used in the treatment of different kind of tract infections such as in urogenital, gastrointestinal and respiratory apparatus, as well as for prevention of these diseases. Bacteria may develop insensitiveness to sulphonamides by various acquired resistance ways. For example, by adopting an alternative pathway in the foliate metabolism, producing enzymes which degrade the antimicrobial drug or expressing the efflux system which prevents the drug to reach the target site of action (Tačić et al., 2017). Many papers in literature have confirmed the bacterial resistance against some sulphonamide compounds (Henry, 1943; Martinez et al., 2009). As consequence, new effective synthetic molecules or the combination of existing compounds are needed.

Among ABs, sulphonamides are among the most widely used in veterinary medicine. In 2017, sulphonamides were the third group of VABs most used in Europe, reaching 9.2% of the total sale of ABs (EMA, 2019). Although their sales declined by 46% during the period from 2011 to 2017, sulphonamides are repeatedly found in groundwater (Carvalho et al., 2016; Kümmerer, 2009; Yao et al., 2015), surface water (Binh et al., 2018; Carvalho et al., 2016; Kümmerer, 2009; Iglesias et al., 2014; Wei et al., 2011), soil (Conde-Cid et al., 2018; Hou et al., 2015) and manure (Kim et al., 2011; Martınez-Carballo et al., 2007). Some studies also show the potential uptake by plants affecting human health through ingestion (Dolliver et al., 2007; Du et al., 2012; Hu et al., 2010).

Sulphonamide compounds are easily degraded by photolysis and ozonation processes in solution, while hydrolysis and chlorination have application limits.

2.3.2 Sulfamethazine

Sulfamethazine (SMT, also called sulphadimidine) is a synthetic molecule of the sulphonamide class. Its molecular formula is $C_{12}H_{14}N_4O_2S$ (4-amino-*N*-(4,6-dimethylpyrimidin-2-yl)benzenesulfonamide, Figure 12) and the molecular weight is 278.33 g mol^{-1}.

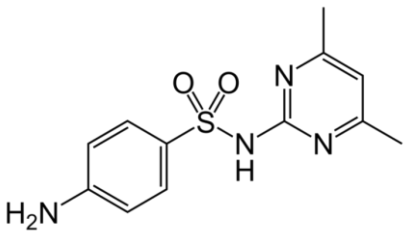

Figure 12. *Chemical structure of Sulfamethazine (SMT)*

Its synthesis was reported firstly by William. T. Caldwell and co-workers at Temple University, Philadelphia, in 1941.

Among the compounds of sulphonamide, SMT is the most frequently used in livestock to treat infections like pneumonia, intestinal infections (especially *Coccidia spp.*), soft tissue infections and urinary tract infections. It is also administered as growth promoter or for disease prevention. The antimicrobial action mechanism is the same of the other sulphonamide compounds, *i.e.* the inhibition of the synthesis of folic acid in cells.

The primary routes of environmental release are direct excretion of urine and manure or after composting to land. The excretion amount for sulfamethazine is up to 90% of the injected one because of the poor absorption in the body (Kim et al., 2011).

There is no evidence in experimental animals for its carcinogenicity to humans (Group 3, IARC). On the other hand, the persistence of SMT in the environment poses a risk to the non-target organisms as well as for the possible development of antimicrobial resistance in bacteria.

In WWTPs, sulphonamides are difficult to decompose by biological methods, such as activated sludge (Garcià-Galàn et al., 2008). This is supported by the fact that the microbial diversity of the sludge culture was significantly reduces by the presence of SMT, which was slightly transformed (Hou et al., 2020). According to the results, *norank-p-Saccharibacteria* was the dominant bacterium in the decomposition of SMT in the wastewater.

Physical-chemical properties and environmental fate of Sulfamethazine

SMT speciation changes with pH. The p*K*a values, 2.65 and 7.65, indicate that this compound exists mostly in the neutral and anion forms under typical environmental conditions (Figure 13).

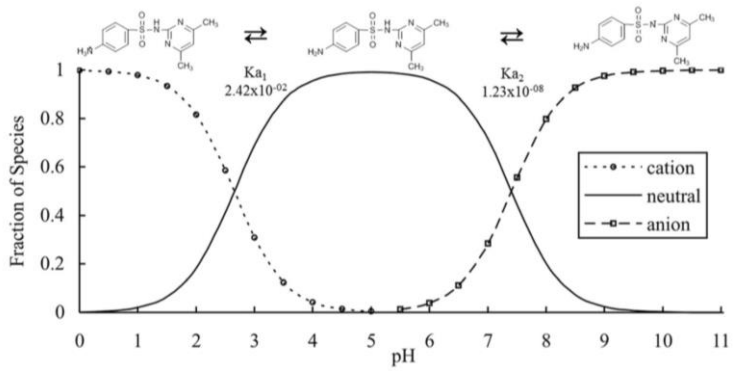

Figure 13. *Distribution of sulfamethazine species by pH (Wegst-Uhrich et al., 2014)*

The fate of SMT in the environment is influenced by the physical-chemical and biological reactions between the compounds, soils and microorganisms. Table 3 reports the principal physicochemical properties of the compound.

Table 3. *Principal physicochemical properties of sulfamethazine*

Parameter	**Value**	**Reference**
Water solubility	1500 mg L^{-1} (pH = 7; 29°C)	The Merck Index (1983)
Melting point	198.5 °C	EPA DSSTox
Vapour pressure	6.82×10^{-9} mmHg (25 °C)	EPA, Estimation Program Interface (2012)
Density	1.4655 g cm^{-3}	Sukul et al. (2006)
Henry's law constant	3.09×10^{-11} Pa m^3 mol^{-1} (25°C)	University of Hertfordshire, VSDB
Partition coefficient (log K_{ow})	0.14 (pH = 7) 0.89	Takacs-Novak et al. (1995) Tolls (2001)
Soil adsorption coefficient (K_d)	0.58-3.91 L kg^{-1} (pH = 5.5) 0.23-1.16 L kg^{-1} (pH = 9)	Lertpaitoonpan et al. (2009)
Organic-carbon distribution coefficient (K_{oc})	86.9-139.7 L kg^{-1} (pH = 5.5) 30.4-47.8 L kg^{-1} (pH = 9)	Lertpaitoonpan et al. (2009)
UV absorption maxima in aqueous solutions	240 nm (ε = 1.7×10^4 L mol^{-1} cm^{-1}) 263 nm (ε = 1.8×10^4 L mol^{-1} cm^{-1}) (pH = 6.1)	Nassar et al. (2017)

SMT is an amphoteric compound that is soluble, exhibiting high environmental mobility. Its low vapor pressure and log K_{ow} cause it to be not volatile and not accumulated by biota. Due to the low K_d, the adsorption on soil is not efficient and it generally decreases by increasing pH, according to the molecule's speciation. By increasing the amount of dissolved organic matter, SMT can be desorbed from soil due to the K_{oc} and the association of the molecule with the dissolved organic matter can facilitate the transport in the environment (Tolls, 2001). Furthermore, anionic SMT may be repelled by the increased surface charge occurring from the dissolved organic matter (Chua et al., 2013). The degradation of SMT in the environment is affected by the initial concentration, the temperature, the solution pH, the type of soil (% OC), the presence of sunlight radiation and microbial activity. Typical values of half-life for SMT at different conditions are reported in Table 4.

Table 4. *Half-life values of sulfamethazine for different remediation processes*

Degradation process	Value of half-life	References
Hydrolysis	~ 1 year at 25°C	Biošić et al. (2017)
Aerobic degradation in manure-amended soils	1.2 to 4.1 days (0.5-50 mg Kg^{-1} SMT)	Lertpaitoonpan (2008)
Anaerobic degradation in manure-amended soils	2.3 to 9.1 days (0.5-50 mg kg^{-1} SMT)	Lertpaitoonpan (2008)
Photodegradation in manure-bacterial suspension	~ 1.8 h (14 mg Kg^{-1} SMT)	Conde-Cid et al. (2018)
Photodegradation in Milli-Q water	~ 32.5 h at pH = 5.5 (14 mg kg^{-1} SMT)	Conde-Cid et al. (2018)

Based on data reported in Table 4, hydrolysis is not expected to be an important degradation path of SMT. This result agreed with that obtained by other authors as Conde-Cid et al. (2018), suggesting that this molecule can persist in waste- and ground-water for a long time.

The degradation in soil of sulphonamides has been studied by many researches, but the results are contradictory. Some studies reported that sulphonamides are not easly biodegradable, while other authors have observed biodegradation. These divergences can be attribuited to differences in the microbial activity of the matrix, to the inoculum, or to differences in the methods used to evaluate biodegradation (Baran et al., 2011). In the cited study of Lertpaitoonpan (2008), the degradation of SMT was relevant under both aerobic and anaerobic conditions. Addition of manure resulted in faster disappearance of SMT, which can be explained by the increase of microbial population and the formation of bounds with the organic carbon. SMT concentrations higher than 50 mg kg^{-1} might carry out an inhibitory effect on the microbial respiration, thus slowing down the degradation; unless under aerobic conditions, in which microbes eventually become acclimatized to the SMT (Lertpaitoonpan, 2008).

On the other hand, a photolysis based on the interaction between the compound and sunlight constitutes the main removal mechanism of SMT in the environment. The photodegradation of this compound in aqueous solution is very efficient, in terms of hours (Conde-Cid et al., 2018). A comparison between two different studies showed that a mixture of SMT in a poultry manure bacteria suspension (Conde-Cid et al., 2018) irradiated by sunlight degrades faster than in a manure-amended soil without light (Lertpaitoonpan, 2008). This suggests that on the soil surface, where the exposition to light is higher, SMT is degraded faster than on the portions below.

Ozonation has been also reported to be highly effective at achieving SMT degradation, more in Milli-Q water than in wastewater (Ben et al., 2012).

Toxicity of sulfamethazine on aquatic organisms

In the last years, many studies about ecotoxicity effects of SMT have been focused on aquatic life because of its high water solubility (1500 mg L^{-1} at 29°C and pH = 7). Researchers have found that SMT can induce toxic effects on algae, which appeared to be the most sensitive organism, followed by invertebrates, like *Daphnia sp.*, and fish (Ji et al., 212). Kim et al. (2007) found that the acute median effective concentrations by luminescence inhibition in *Vibrio fischeri* is EC_{50} = 303.0 mg L^{-1} and EC_{50} = 344.7 mg L^{-1} for 5 and 15 min duration test, respectively. SMT also displayed little or no evidence of phytotoxicity in *Lemnia gibba* for any endpoints measured in the selected concentration range except wet mass, that shows an EC_{50} = 1.277 mg L^{-1} for 7 days duration test (Brain et al., 2004). Anyway, exploitation of SMT antibiotics may be harmful to organisms initially less likely to be reached by it. For example, Reybroek et al. (2010) reported SMT in honey as result of the presence of AB residues in beeswax after the treatment.

European legislation concerning Sulfamethazine

SMT is a short-acting sulphonamide, usually administered in combination with other compounds and sold as a powder for oral use. Its identification CAS number is 57-68-1, while the European Community (EC) number is 200-346-4. It can be found on the market also as sodium sulfamethazine under the names of Bovibol, Sulmet and Vesadin.

The European Union Commission Regulation No 37/2010 sets the maximum residues limit (MRL) for all sulphonamides, included SMT, to 100 μg kg^{-1} for muscle, fat, liver, and kidney from all food-producing species and bovine, ovine, and caprine milk. Their use is prohibited for animals that produce eggs for human consumption. In the case of more than one sulphonamide, the sum of each compound should not exceed the provided MRL value. Honeybees are also considered food-producing species.

The monitoring of SMT is inserted in the European Union Council Directive 96/23/EC regarding "substances and residues thereof in live animals and animal products", in which SMT belongs to Group B. For Group B substances, surveillance should be aimed particularly at controlling the compliance with MRLs for residues of veterinary medicinal products fixed in Annexes I and III to Regulation (EEC) No 2377/90, and the maximum levels of pesticides fixed in Annex III to Directive 86/363/EEC, and monitoring the concentration of environmental contaminants (Council Directive, 96/23/EC).

Regarding human exposure, the Joint FAO/WHO Expert Committee on Food Additives (JECFA) in 1994 established an acceptable daily intake (ADI) of 0-50 μg kg^{-1} bw, while no carcinogenic effects was evidenced.

So far, legal limits have been established for SMT in food, but there is no legislation applied to environmental matrices. However, although the low concentrations do not exceed any current water standards, they are sufficient to cause adverse effects.

2.3.3 State of art concerning sulfamethazine in AOPs

Many studies have been carried out in the last years about AOPs applied to the degradation of SMT in water and wastewater. The different experimental set ups may vary in effectiveness of the mineralization and in the formed byproducts.

Many studies agreed on common pathways, although the intermediates can vary depending on the experimental conditions. The SO_2 elimination from SMT through direct photolysis is a typical photodegradation step by forming the 4-(2-imino-4,6-dimethylpyrimidin-1(2H)-yl)aniline compound (Boreen et al., 2005). The •OH radicals, deriving from AOPs, are able to generate diverse hydroxylated products, which differ from the position in the molecules. They can also attack the heterocyclic ring, resulting in its opening (Babić et al., 2015). Both SO_2 removal and •OH addition may lead to the formation of a photoproduct, 4,6-dimethylpyrimidin-2-amine, which represents the pyrimidine part of SMT. Ge et al. (2019) found that, as well as •OH, the addition of singlet oxygen species $^1O_2$ to the amino-N group can contribute to the photodegradation of SMT. Further hydroxylation could induce the cleavage of C-S and N-S bounds, thereby generating lower molecular mass photoproducts and leading ultimately to the full mineralization of these compounds into CO_2, H_2O and other possible inorganic compounds.

Regarding direct photolysis, Adams et al. (2002) demonstrated that the degradation of SMT with UV-C dosages at 254 nm, in order of 30 to 3000 mJ cm^{-2}, achieved a value between 50 and 80% both in distilled/deionized water and in river water. These results show that UV photolysis alone is not a viable way of removing the molecule, but combined AOPs, such as UV/VUV (Li et al., 2017; Babić et al., 2015), UV/TiO_2 (Kaniou et al., 2005), UV/Cl_2 (Xiang et al., 2019), UV/$S_2O_8^{2-}$(Gao et al., 2012), or UV/H_2O_2 (Zhang et al., 2016), can make the transformation much more efficient.

Babić et al. (2015) observed a complete removal of SMT occurred in ultrapure water under VUV/UV-irradiated solution at 185/254 nm over a period of 60 min, while no degradation was observed in the solution irradiated with UV-A at 365 nm within 120 min time. The low

efficiency of UV photolysis alone opposed to the higher degradation rate of the VUV/UV system was also confirmed by Li et al. (2017). They also highlight the pH dependence of SMT degradation by affecting the absorbance and quantum yield values, showing its maximum at pH 7.5. Therefore, the neutral species is the most reactive in the VUV/UV process. Six byproducts were identified, but a low detected amount of inorganic anions (SO_4^-, NO_3^-, and NO_2^-) and a high Total Organic Carbon (TOC) revealed that most of the organics was still retained in the byproducts, together with a possible residual antibacterial activity. Degradation of sulphonamides, including SMT, via reaction with •OH was widely analyzed (Sági et al., 2015). Depending on the case, inorganic ions and organic matter can affect the degradation rate both in a positive or negative way. For example, experiments showed that the photolysis of SMT increased with the increase in Cl^-concentration, while NO_3^- had a double effect: it could decrease the degradation rate of SMT due to the absorption in the same range or enhanced the reaction thanks to the production of reactive species (*i.e.*, •OH, NO_2•) via sensitization effects (Yi et al., 2018). The same ambiguous effect was evidenced for fulvic acids (FA). Some authors found that the excited states of FA further induced the degradation of organic compounds (García-Galán et al., 2012), while others noticed that the competition for photons and the quenched by dissolved oxygen of the excited FA states inhibited the photolysis rate (Yi et al., 2018). Turbidity can also act as a shelter screen for light, decreasing photodegradation for SMT as well for other pollutants (Thiele-Bruhn, 2003; Conde-Cid et al., 2018).

Among different AOPs, ultrasonic irradiation is relatively new and has been tested for SMT degradation by Gao et al. (2013). The transformation rate of SMT during sonolytic degradation was slightly inhibited by the presence of some anions (NO_3^-, Cl^-, SO_4^{2-}) in water, but significantly improved by the presence of $HCO_3^-$and Br^-.

Combination of photolysis with H_2O_2 as auxiliary oxidant could enhance the SMT degradation (Babić et al., 2015; Zhu et al., 2019).

Heterogeneous photocatalysis using TiO_2 demonstrated quantitative degradation of the organic molecule in 4h (Kaniou et al., 2005). Transformation rate increased with TiO_2 loading. Similar trends were found for photo-Fenton processes, which showed high performance in removing the contaminant. Pérez-Moya et al. (2010) evidenced an increase in the toxicity of the solution during the inizial degradation reaction of a photo-Fenton process. Most of the sulphonamide's transformations follow pseudo-first order kinetic model during photolysis (Conde-Cid et al., 2018; Xiang et al., 2019) in laboratory-scale tests.

Furthermore, SMT transformation was carried out by ozonation process which proved to be the most effective method among all AOPs (Gome et al., 2012; Garoma et al., 2010). A reaction time of 1.3 min was sufficient to transform 0.05 mg kg^{-1} SMT in a prefiltered river water sample at pH 7.5 using 0.3 mg L^{-1} ozone dose. The reaction was even faster in distilled/deionized water (Adams et al., 2002). In wastewater, the degradation rate by ozonation was lower, but SMT was completely removed within 20 min anyway (Lin et al.). According to many studies, ozonation for sulphonamide compounds fits a second order kinetic model in laboratory-scale tests (Ben et al., 2012; Ikehata et al., 2006).

The O_3/UV configuration did not show any significant improvement in removal of SMT compared to the simple ozonation, while the addition of H_2O_2 on the contrary was the most efficient for SMT removing according to Svestkova et al. (2019).

3. Goals of the thesis

The aim of this thesis work was the investigation of various AOPs for the elimination of sulfamethazine (SMT), a widely used veterinary antibiotic, from aqueous solution. The methods were ozonation, its combination with UV (254 nm) photolysis and UV/VUV (254/185 nm) photolysis. The effect of various reaction parameters on the rate of transformation, mineralization, ecotoxicity, reaction pathways and electric energy consumption were studied.

In the first part of experimental work the effect of basic parameters, such as dissolved O_2, O_3 dosage, initial concentration and pH, was studied on the transformation rate of SMT.

Using UV/VUV photolysis and ozonation, •OH can form. The relative contribution of the •OH based reaction to the transformation of SMT was studied via addition of terc-buthanol (TBA), which is a well-known •OH scavenger.

The formed products were identified by HPLC-MS, using SPE as sample pre-treatment method. Based on the intermediates formed, reaction mechanisms can be suggested for the transformation, including the role and contribution of various reactive species.

During the transformation of SMT, the changes of Chemical Oxygen Demand (COD), Total Organic Carbon (TOC) content, H_2O_2 concentration and NO_3^- concentration were monitored.

When the elimination of an antibiotic or any other toxic component is investigated, there is a possibility that toxic intermediates form in its place. The change of ecotoxicity during photocatalytic treatment is followed by using ecotoxicity test based on *Vibrio fischeri* test organism.

From the point of view of practical application, the effects of the matrix on the efficiency and energy consumption must be investigated. This work involves examining two mild matrices (drinking water and purified industrial wastewater) for the efficiency of applied method. The comparison of the energy consumption of the methods was based on the calculation of Electric Energy per Order.

4. Materials and Methods

4.1 Standards and Reagents

The analytical standards for sulfamethazine (SMT, ≥ 99%) were obtained from Sigma-Aldrich®. The HPLC grade Methanol (MeOH), the formic acid (99-100%), NaCl (99%), NaOH (99%) and HCl solution were obtained from VWR® (HiPerSolv CHROMANORM®). Ultrapure water was prepared with a Milli-Q® Integral Water Purification System (MerckMillipore®). The O_2 (99.5%), N_2 (99.995%) and air were provided by Messer Hungarogáz Kft.

Various matrices, such as drinking water from Szeged (Hungary), and industrial wastewater (purified by biological treatment and reverse osmosis) were used. The parameters are presented in Table 5.

Table 5. *Parameters of the matrices*

Parameter	Drinking water	Purified wastewater
pH	7.8	7.2
Conductivity (µS cm^{-1})	627	22
COD (mg dm^{-3})	4.2	2.9
NH_4^+–N (mg dm^{-3})	< 0.4	< 0.4
NO_3^- (mg dm^{-3})	< 0.7	1.5
Cl^- (mg dm^{-3})	8.75	< 1.0
TOC (mg dm^{-3})	0.79	0.11
Inorganic carbon* (mg dm^{-3})	73.4	3.1

*sum of the concentration of HCO_3^-, CO_3^{2-} and dissolved CO_2

4.2 Light Sources and Experimental Apparatus

Two low-pressure mercury vapour (LP) lamps (GCL307T5/CELL and GCL307T5VH/CELL, 227 mm arc length, both produced by LightTech) were used for UV (254 nm) and UV/VUV (254 nm/185 nm) irradiations. The parameters (electrical power 15 W and UVC-flux power 4.3 W; diameter: 20.5 mm, length: 307 mm) of both lamps were the same. The envelope of the UV lamp emitting at 254 nm was made of commercial quartz, while the UV/VUV lamp's envelope was made of synthetic quartz to be able to transmit the VUV photons. The flux of 254 nm photons (5.97×10^{-6} mol photon s^{-1}) of both lamps (UV and UV/VUV) was determined by ferrioxalate actinometry (Hatchard et al., 1956) and found to be the same (Alapi et al., 2007). The relative radiant power efficiency of the 185 nm VUV light is about 6-8% compared to the 254 nm emission.

The photochemical experiments were carried out in a 500 mL cylindrical glass reactor having 60 mm inert diameter and 300 mm height. The optical path length was 20 mm, which is enough for the total absorption of 185 nm light (Mora et al., 2018). The reactor was thermostated at room temperature (25±1 °C). A gas filter was installed in the bottom of the reactor to bubble the finely divided gas bubbles thought the total volume of the treated solution. The aqueous solutions were continuously bubbled through this gas dispersing system with oxygen, air, nitrogen or oxygen/ozone mixture to set various dissolved oxygen or dissolved ozone concentration. Before measurement the solution was boubled with oxygen or nitrogen for 20 min. Dissolved O_2 concentration was 40.0 mg L^{-1} in the case of O_2 saturated solutions, while in the case of N_2 boubbling its concentration was less than 0.6 mg L^{-1}. During the ozonation, O_3 gas was supplied by Ozomatic Modular 4HC type ozonizator, using O_2 as feeding gas with flow up to 500 mL min^{-1}. The reaction was started with turning on the light source or ozonator. The experimental setup is chemically depicted in Figure 14.

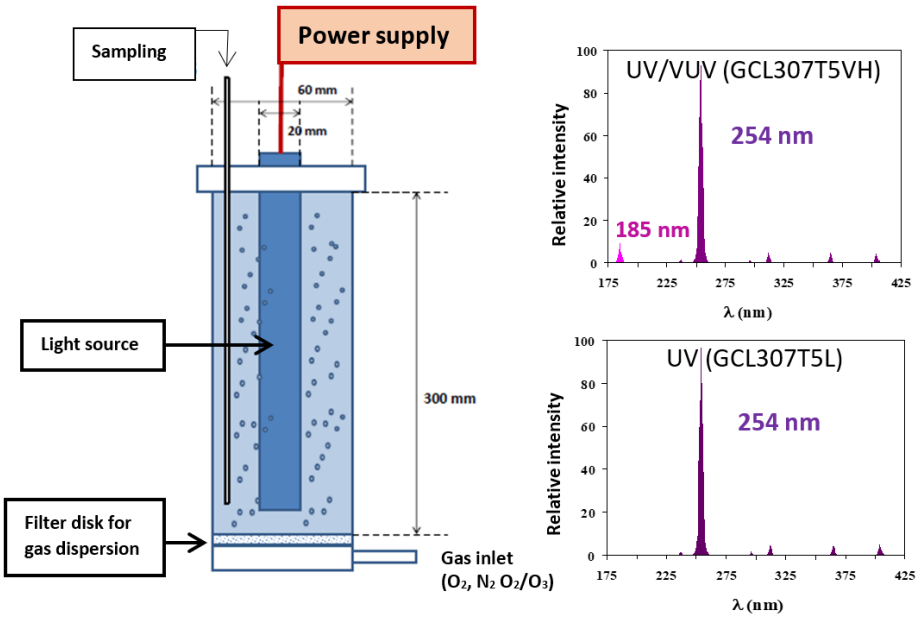

Figure 14. *Experimental setup and the spectra of the light sources*

4.3 Analytical methods

The concentration of SMT stock solution was measured by spectrophotometry. Spectrophotometric measurements were made with an Agilent 8453 UV-Vis spectrophotometer (Figure 15), using 0.20, 0.50 and 1.00 cm path-length cuvettes. Samples were taken after 0, 1, 2, 3, 4, 5, 10, 15, 20, 25, 30, 40, 50, 60, 70, 80, 90, 105, 120 minutes treatment. The concentration of O_3 was also determined spectrophotometrically, using a flow-through gas cuvette having 1.00 cm path-length.

https://spwindustrial.com/agilent-hp-8453-uv-visible-spectrophotometer-g1103a-with-computer-chem-sw/

Figure 15. *Configuration of an Agilent 8453 UV-Vis spectrophotometer*

The spectra of SMT and O_3, together with the main characteristic wavelengths, are shown in Figure 16.

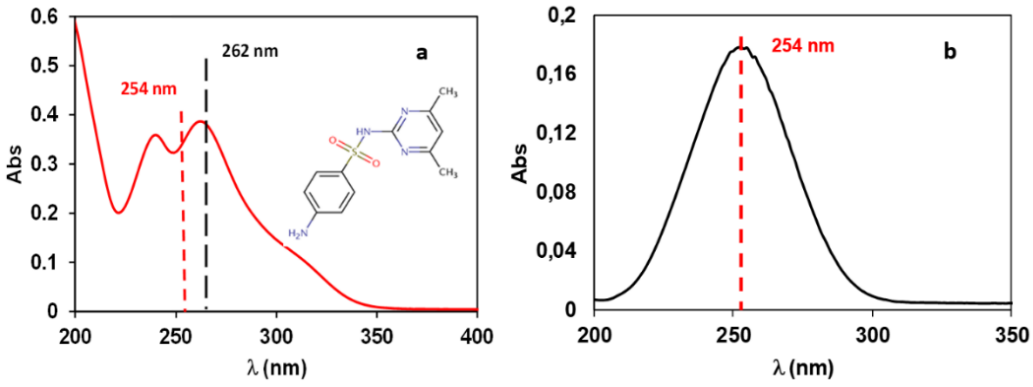

Figure 16. *Spectra of sulfamethazine (a) and O_3 (b)*

The samples were also analysed using an Agilent 1100 HPLC coupled with a diode array detector (DAD). The column (Lichrospher 100, RP-18; 5 µm) was thermostated at 25°C, the flow rate of eluent was 1.0 cm^3 min^{-1}, and 20 µL sample was injected. Two

chromatographic methods were developed: the eluent of “Fast method” was a methanol-water solution (with 1% HCOOH) = 30:70 (v/v) mixture, while the “Slow method” had a lower percentage of methanol, 25:75 (v/v). The detection was performed at 262 and 210 nm. Under these conditions, SMT was eluted at 9.0 min with the Slow method and 5.0 min with the Fast method.

SMT was characterized by an initial rate of transformation, obtained from linear regression fits to the concentration-time plot, equal to up to 25%. Some experiments were repeated three times to check the reproducibility of the experimental results. The accuracy of the initial transformation rates was within ±7%.

The identification of intermediates was performed using an Agilent LC/MSD VL mass spectrometer coupled to the HPLC device (Figure 17).

Figure 17. *Configuration of an Agilent LC/MSD VL mass spectrometer coupled to the HPLC device*

For HPLC-MS analysis, solid phase extraction (SPE) was used as sample pretreatment method. The MS measurements were performed using negative electrospray ionization (ESI) mode, capillary voltage was 3.0 kV, drying gas temperature was 300°C, and the fragmentor voltage was 70 V. The scanned mass range was between 50 and 500 AMU.

The ElectroSpray Ionization (ESI) source is an Atmospheric Pressure Ionization (API) technique, in which the ionization is produced when a strong electric field is applied on a liquid passing through a capillary. This electric field is formed applying a potential difference (3-4000 V) between the capillary and the counter electrode. The molecules have to be already present is the solution as ions in order to achieve the ionization; formic acid in the HPLC-MS eluent allowed their formation in the solution. Assisted by a sheath gas, the solvent evaporates from a charged droplet until it becomes unstable upon

reaching its Rayleigh limit: this occurs when the surface tension can no longer sustain the electrostatic repulsion, causing the droplet deformation. Then, the droplet undergoes Coulomb fission, whereby it explodes creating many smaller, more stable droplets. The process of solvent evaporation and Coulomb fission occurs repeatedly (Figure 18). The passage from charged droplets to gas-phase ions occurs through two mechanisms, depending on the molecular weight of the droplets: the Ion Evaporation and the Charge Residue mechanism.

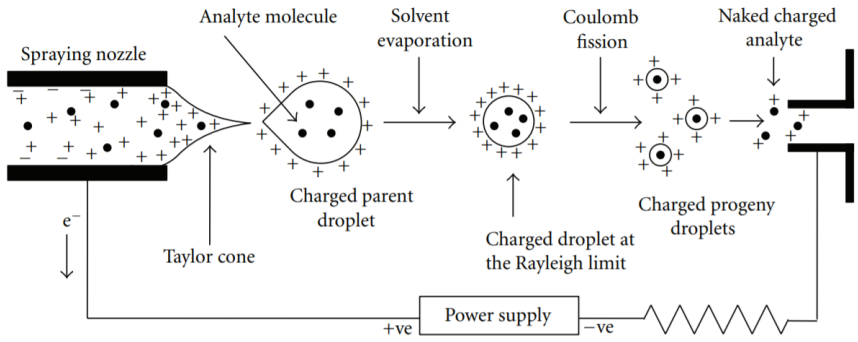

Figure 18. *Schematic representation of the electrospray ionization process (Banerjee et al., 2012)*

Generally, a negative ESI source generates deprotonated ions $(M\text{-}H)^-$; for macromolecules (not in this case) also multiply charged ions $(M\text{-}nH)^{n-}$ can be observed, together with adducts $(M\text{-}H+Na)^-$ by the addition of cations present in the solvent or in the air.
Acids, phenols, nitro compounds are easily ionized in the negative ionization mode by ESI (Schug, 2012).

4.4 Analysis of key parameters

4.4.1 Nitrate test

The colorimetric test kits provided by Merck-Millipore, coupled with a Spectroquant® Multy Vis-spectrophotometer, was used to determine the concentration of NO_3^- (DMP method, 0.10-25.0 mg dm^{-3} NO_3^--N). In a sulfuric and phosphoric solution, the NO_3^- reacts with 2,6-dimetilphenol (DMP), forming the compound 4-nitro-2,6-dimetilphenol, which is determine by photometry. The procedure consisted in adding sequentially: 4 ml of reagent 1, 0.5 ml of pretreated sample (5-25°C), and 0.5 ml of reagent 2. The pH of each pretreated sample must be within the range 1-3 by adjusting it with sulfuric acid (H_2SO_4).

The solutions could be mixed only when all the reagents were added, and the reaction time was 10 min long. The colour of the solution remains stable for 30 min after the end of the reaction time (after 60 min the measurement value would increase by 5%).

The standards were analysed at 335 nm, where NO_3^- absorbs, while samples were analysed at 350 nm because of the overlapping with the SMT absorption spectrum. The measuring range of the NO_3^- test is between 4.4 and 110.7 mg L^{-1} of NO_3^- for a 1.00 cm path-length cuvette.

The standard solutions were prepared from a stock solution of sodium nitrate ($NaNO_3$) 10091 mg L^{-1}. Two calibration curves were made: the first one to test the method and to find the suitable range, the second one was the definitive calibration. In the latter, the maximum concentration of nitrogen (N) was around 25 mg L^{-1} when the SMT concentration was 10^{-4} mol L^{-1}. Table 6 reported the standard concentration of NO_3^- used for the calibrations.

Table 6. *Concentrations of nitrate to perform the range finding and the definitive calibration*

Flask (100 ml)	**Range finding calibration**	**Definitive calibration**	**Range finding calibration**	**Definitive calibration**
	$NaNO_3$ concentration (mg L^{-1})		**NO_3^- concentration** (mg L^{-1})	
C1	0	0	0.00	0.00
C2	20	5	14.49	3.64
C3	40	10	28.90	7.22
C4	60	15	43.35	10.93
C5	80	20	57.79	14.58
C6	100	25	72.24	18.22
C7		30		21.68

One sampling was made with UV/VUV lamp. The concentration of SMT was 10^{-4} mol L^{-1} and the samples were taken at 0, 2, 4, 6, 8, 10, 15, 20, 30, 40, 50, 60, 80, 90 min time.

4.4.2 Hydrogen Peroxide test

The colorimetric test kits provided by Merck-Millipore, coupled with a Spectroquant® Multy Vis-spectrophotometer, was used to determine the concentration of H_2O_2 (0.015-6.00 mg dm^{-3}). In the presence of a phenanthroline derivative, hydrogen peroxide reduced copper(II) ions to copper(I). In the process these ions form an orange-coloured complex that is determined photometrically. The procedure consisted in adding sequentially: 2.0 ml of Milli-Q to dilute the solution, 2.0 ml of sample, 0.25 ml of test 1

and 0.25 ml of test 2 reagents. The pH must be within the range 4-10 for the achievement of the reaction and the measuring range was between 0.02 and 5.50 mg L^{-1} H_2O_2. The solutions were left to stand for 10 min, and then measured in the photometer.

4.4.3 Total Organic Carbon and Chemical Oxygen Demand analysis

The mineralization was followed by Total Organic Carbon (TOC) measurements performed with TOC Analytik Jena multi N/C 3100-type instrument. Potassium hydrogen phthalate was used for the calibration.

The Chemical Oxygen Demand (COD) measurements were performed using colorimetric test kits (LCK1414, Hach Lange Ltd.) and DR 2800 (Hach) Vis-spectrophotometer. Samples were treated for 2 h at 148 °C (HT200S).

4.4.4 pH analysis

The pH was measured with an InoLab pH 730p pH-meter.

4.5 Solid Phase Extraction

A Solid Phase Extraction (SPE) was used as sample pretreatment method to isolate and concentrate our analyte from the solution. The cartridge for neutral compounds was selected referring to the properties of SMT and its possible intermediates. A 5 steps procedure was applied in the following sequence:

1. Conditioning: 2.0 ml methanol
2. Equilibration: 2.0 ml water
3. Loading: 50 cm^3 sample
4. Washing: 2.0 ml water
5. Elution: 1.5 ml methanol

The extracted samples were analysed by HPLC-MS.

4.6 Ecotoxicity Test

Ecotoxicity tests based on the bioluminescence measurements of marine bacteria *Vibrio fischeri* (*V. fischeri*) was applied to provide information on acute toxicity of the multicomponent solution formed during various treatments (Figure 19).

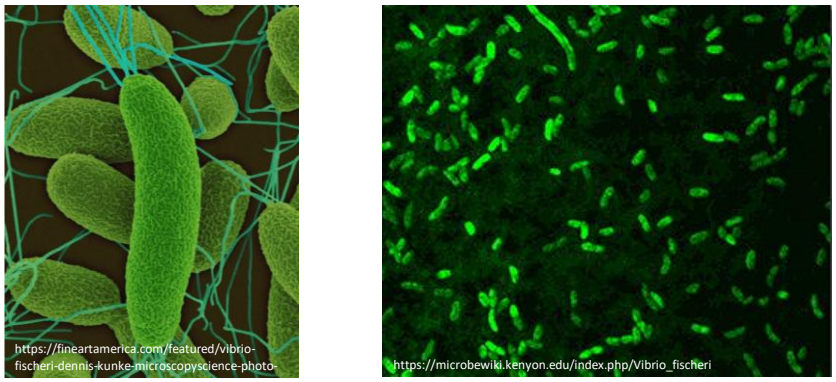

Figure 19. *Vibrio fischeri bacteria (left) and its bioluminescence (right)*

The LCK480 tests were provided by Hach-Lange. The pH and NaCl concentration of each sample were adjusted to 6.5-8.0 and 2.0% w/v, respectively. H_2O_2, which was formed during the transformation of organic substances, was decomposed in the samples by adding catalase enzyme (Sigma Aldrich, 2000-5000 unit mg^{-1}) before starting the ecotoxicity test. The enzyme concentration in the samples was adjusted to 0.20 mg dm^{-3}. The inhibition of bioluminescence was measured using a Lumistox 300 (Hach Lange) luminometer after 15 min incubation time. The control sample was purified water containing 2.0% w/v NaCl, while the standard (50±10% inhibition) solution contained 7.5% w/v NaCl.

4.7 Electric Energy per Order (E_{EO})

The comparison of the methods is generally based on the transformation rate of the target substance, or on the total organic carbon content. In addition to these techniques, the applied methods of Electric Energy per Order (E_{EO}) calculations is also compared. The calculation of the E_{EO}, which is usually applied for solutions with low initial substrate concentrations, enables the economic comparison of the different irradiation techniques. It represents the amount of electric energy required for reduction of the target compound concentration in a unit volume (*i.e.*, 1 m^3) by one order of magnitude (Bolton et al. 2001).

In batch operation E_{EO} values (kWh m^{-3} $order^{-1}$) can be calculated using the following equation:

$$E_{\mathrm{EO}} = \frac{P \times t \times 1000}{V \times \lg(c_i/c_f)}$$

where P is the rated power [kW] of the AOP system, V is the volume [L] of water, t is the treatment time [h], c_i and c_f are the initial and final concentrations [mol L^{-1}], respectively, of the compound investigated. Factor 1000 converts L to m^3.

5. Results and Discussion

5.1. Transformation of sulfamethazine via UV and UV/VUV photolysis

Before starting the measurements of SMT transformation by UV and UV/VUV photolysis, a 5-points calibration at 262 nm has been done (Figure 20).

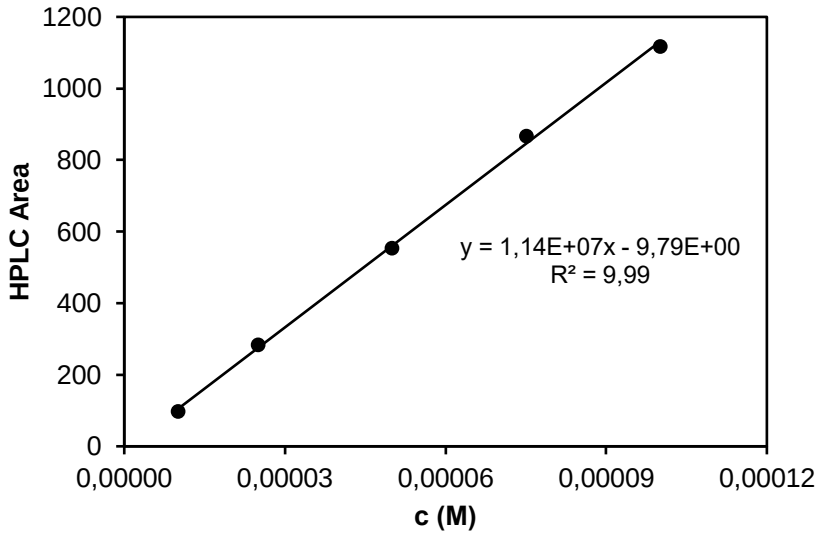

Figure 20. *Calibration curve of sulfamethazine measured with HPLC-DAD for UV and UV/VUV photolysis*

5.1.1. Effect of initial concentration

Efficiency of UV photolysis is determined by the wavelength of the light source, the molar absorbance of the substrate at the wavelength emitted by the light source and the quantum yield of the transformation (number of the transformed molecule divided by the number of the absorbed photon). Molar absorbances of SMT were found to be ε_{254nm} = 17550 M^{-1} cm^{-1} at 254 nm and ε_{265nm} = 19460 M^{-1} cm^{-1} at 265 nm, in agreement with the data presented in the literature (Battista et al., 2014; Li et al., 2017), and it was calculated from the slope of the calibration curve divided by the path-length of the light (Figure 21).

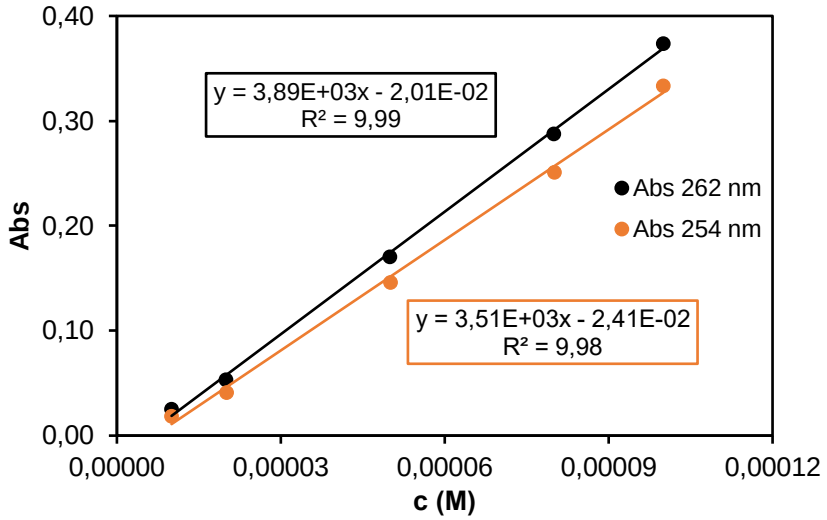

Figure 21. *Spectrophotometric calibration curve of sulfamethazine at 262 and 254 nm*

According to the Lambert-Beer law, from the value of the molar absorbance of SMT, its initial concentration and geometric parameter of the reactor (irradiated layer of the solution was 20 mm), the absorbance of the treated solution at 254 nm can be calculated. As Figure 22 shows, in the case of the UV photolysis the intensity of the absorbed UV light increased with increase of the initial concentration. Above 5.0×10^{-5} M initial concentration, the UV light was absorbed completely within 20 mm. This is the reason of why, above this concentration, the transformation rate does not increase further with the concentration of the SMT. Using the photon flux emitted by the LPM vapour lamp and the transformation rate of SMT, the quantum yield of the transformation was calculated. The obtained value was 0.018, which is a good agreement with the quantum yield reported by Li et al. (2017).

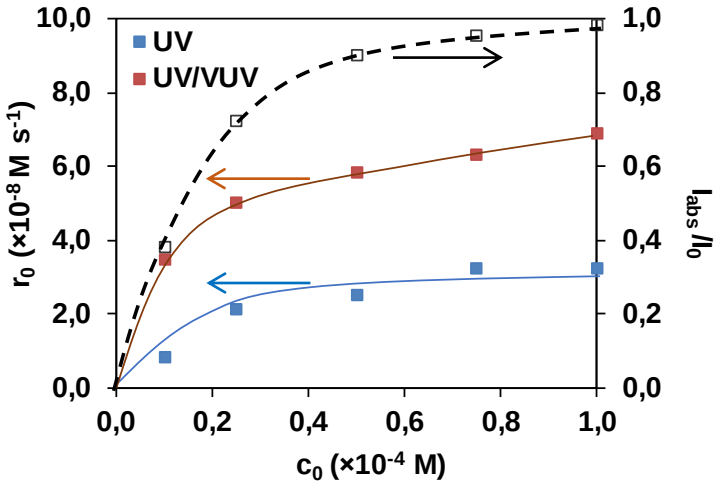

Figure 22. *Transformation rate of sulfamethazine and its absorbance at 254 nm versus the initial concentration in UV and UV/VUV irradiated solution, saturated with air*

In the case of UV irradiated solution, the direct photolysis is responsible for the transformation of SMT. In UV/VUV irradiated one, besides direct UV photolysis, there is another possibility of the transformation of SMT. VUV light is absorbed by water, which results in the formation of reactive H• and •OH radicals. Thus, the conversion of SMT can also occur through radical-based reactions. Although the intensity of 185 nm VUV light is one magnitude lower than the intensity of 254 nm UV light, it caused a significant increase of the transformation rate. VUV light is fully absorbed within 11 mm water layer, thus, the formation rate of H• and •OH is constant. Probably the relative contribution of the radical based reaction to the transformation of SMT is higher at lower concentrations. This can explain why the ratio of the transformation rates ($r_0^{UV/VUV}/r_0^{UV}$) determined in UV and UV/VUV irradiated solution results about two times higher value at 1.0×10^{-5} M ($r_0^{UV/VUV}/r_0^{UV}$ = 4.1) than at 1.0×10^{-4} M ($r_0^{UV/VUV}/r_0^{UV}$ = 2.1) (Table 7).

Table 7. *Relative intensity of the absorbed light and the initial transformation rate of sulfamethazine determined in UV and UV/VUV irradiated solution at various initial concentrations*

c_0 ($\times10^{-4}$ M)	$I^{254\ nm}/I_0^{254\ nm}$	UV	UV/VUV	$r_0^{UV/VUV}/r_0^{UV}$
		r_0 ($\times10^{-8}$ M s^{-1})		
0.10	0.38	0.84	3.44	4.1
0.25	0.75	2.08	5.00	2.4
0.50	0.93	2.52	5.82	2.3
0.75	0.96	3.23	6.28	1.9
1.00	0.98	3.20	6.87	2.1

5.1.2. Effect of dissolved O_2

In the case of both UV and UV/VUV photolysis, the effect of dissolved O_2 was investigated (Figure 23). The transformation of SMT was followed in O_2 saturated, O_2-free (solution was bubbled with N_2) and in aerated solutions at 1.0×10^{-4} M initial concentration. In VUV irradiated aqueous solution, dissolved O_2 reacts fast with H•, thus the concentration of reactive species decreases, which can reduce the transformation rate. However, the dissolved O_2 generally has positive effect on the transformation rate because of the formation of peroxyl type radicals from carbon centred radicals (R-C•-R' + $O_2 \rightarrow$ R-C-OO•-R'). The formation of peroxyl radicals opens up new pathways for the transformation and has a crucial role in the mineralization of organic substances. In UV irradiated solution, radicals also can form from organic substances via bound breaking caused by UV photons absorption. Moreover, O_2 is able to enhance the transformation rate when photoionization occurs. Opposite to the possible and often observed positive effects,

dissolved O_2 has a negative effect in the case of UV photolysis, while in the case of UV/VUV photolysis no significant effect was observed. Probably, these two effects (negative effect on UV photolysis and the positive effect on radical based reaction) balance each other out in the case of the combination of UV and VUV photolysis. (Table 8).

Table 8. *Effect of dissolved O_2 on the initial transformation rate of sulfamethazine in UV and UV/VUV radiated solutions*

	O_2	air	N_2
	r_0 ($\times 10^{-8}$ M s^{-1})		
UV	2.69	3.20	3.34
UV/VUV	6.17	6.8	6.38

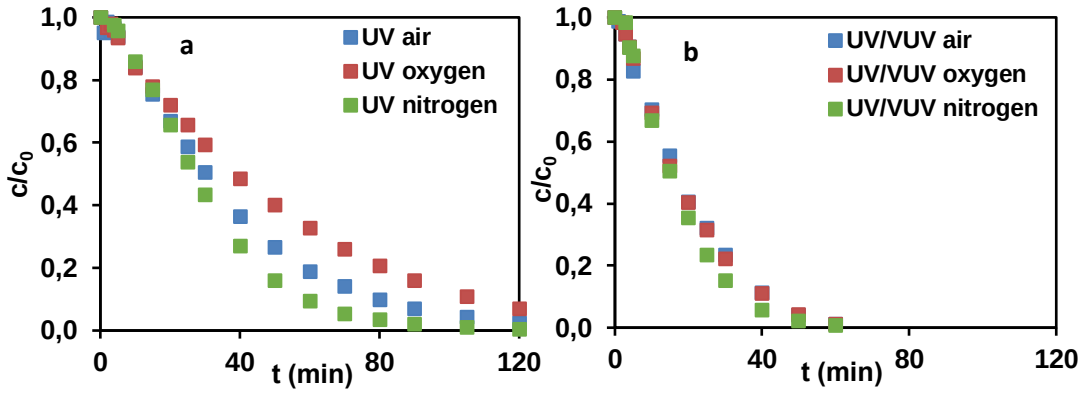

Figure 23. *Effect of dissolved O_2 on the transformation of sulfamethazine (1.0×10^{-4} M) in UV (a) and UV/VUV (b) radiated solutions*

The change in spectrum provides information on the processes taking place in solution during the treatment. Thus, the effect of dissolved O_2 on the shape of the spectra was also studied in each case. If Figures 24a and 24b, representing the spectra of UV radiated solutions, are compared, some significant differences can be observed in dissolved O_2 containing and O_2-free solutions' spectra.

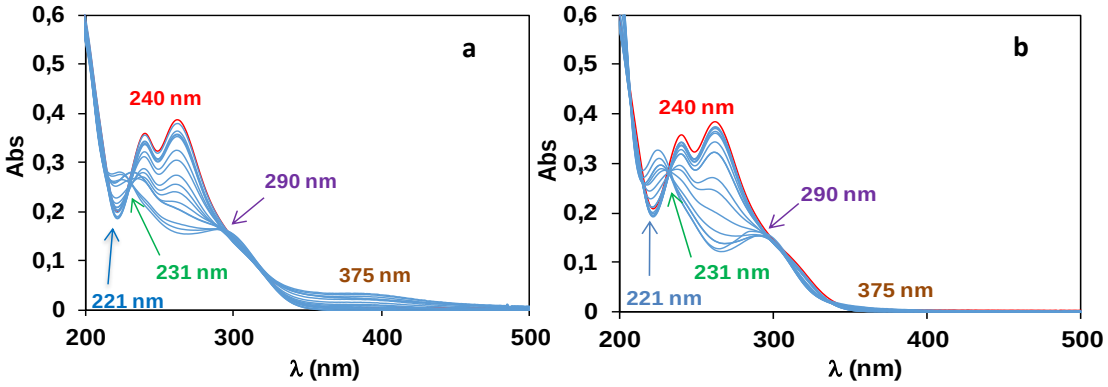

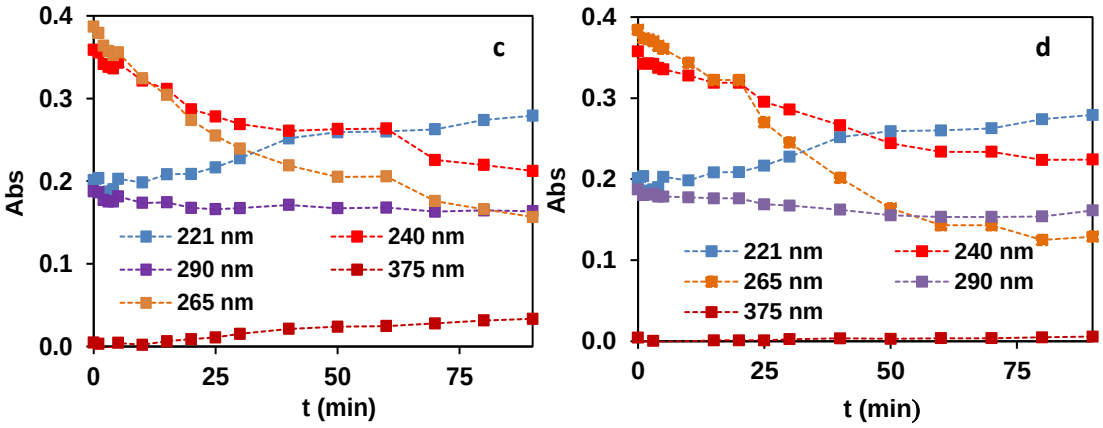

Figure 24. *Spectra of the UV radiated solutions (a: aerated; b: O_2-free) and the absorbance determined at some selected wavelengths (c: aerated; d: O_2-free)*

UV-Vis spectrum of SMT has a double peak in UV range: at 240 and 265 nm. The transformation of SMT versus time of treatment and the change of absorbance at 240 and 265 nm (the characteristic peaks of SMT) presented in the Figure 24 can be correlated. Observation makes it likely that intermediates with the same or similar structure of the parent compound are formed and accumulated during this treatment. Two isobestic points appear at 231 and 290 nm approximately, suggesting the presence of an equilibrium between two species, so that the sum of the concentrations of the two species is constant and only their ratio is variable. Another important change in absorbance takes place at around 375 nm, and it can be observed only in the presence of dissolved O_2. SMT decomposed completely after 120 minutes (Figure 24a), but the spectrum of sample taken at 120 minutes still looks like the SMT's spectrum (Figure 24c), which underlines the insufficient capacity of UV photolysis in transformation of some intermediates having similar spectra (and probably similar chemical structure) than the parent component.

In UV/VUV irradiated solution a large part of SMT transforms via direct UV photolysis. This may explain why the shape and change of the spectral series are very similar for UV and UV/VUV treated O_2-free samples (Figures 24b and 25b). Although dissolved O_2 has no significant effect on the transformation rate of SMT (Figure 23b), its presence highly effects the spectrum (Figure 25a) in the case of UV/VUV photolysis. As mentioned previously, the joint presence of •OH and O_2 opens up new pathways for the transformation of SMT and its intermediates. In this connection, it is noticeable that dissolved O_2 has a much more remarkable effect in the case of UV/VUV than UV treated aqueous solutions.

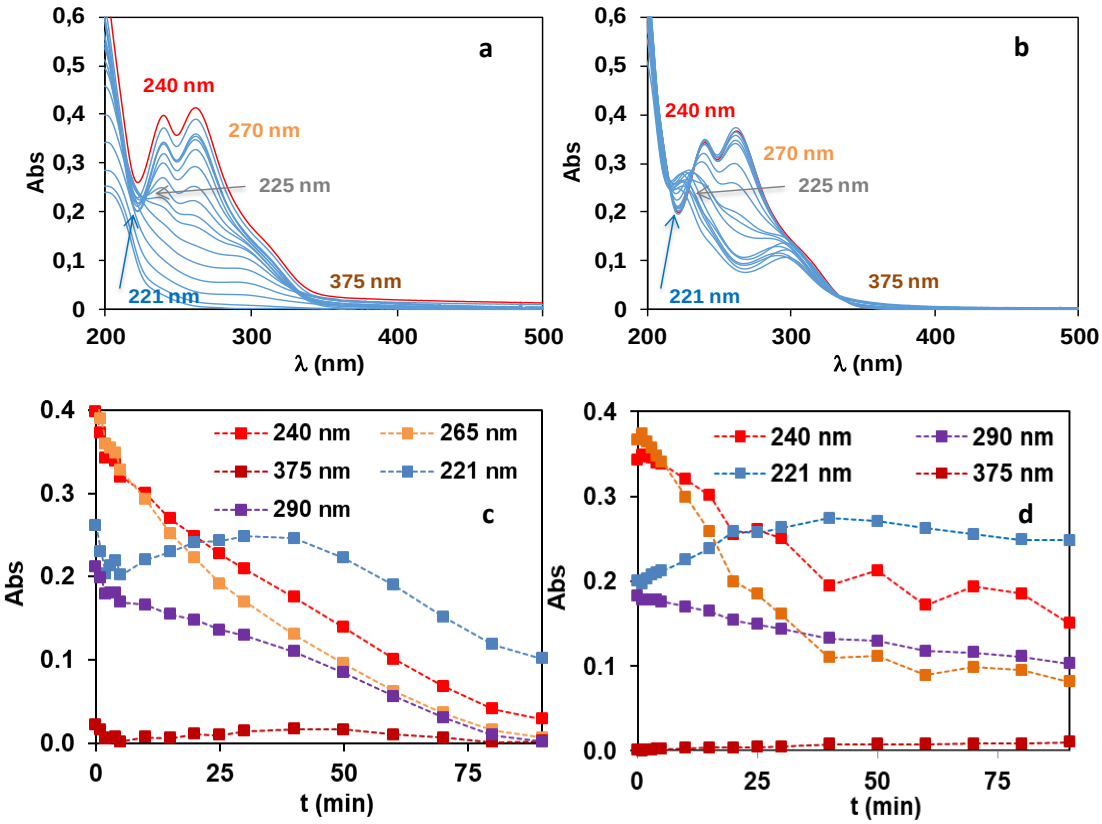

Figure 25. *Spectra of the UV/VUV radiated solutions (a: aerated; b: O_2-free) and the absorbance determined at some selected wavelengths (c: aerated; d: O_2-free)*

Due to the high energy of VUV photons, the absorbance determined at 240 and 265 nm changes faster than during UV photolysis and the accumulation of aromatic intermediates is less significant, *i.e.* their transformation is much more effective. The latter one is proved by the change of the absorbance determined at 221 nm. It increases throughout the duration of UV radiation, while in the UV/VUV irradiated O_2-containing solution, a slight increase followed by an intense decrease is observed. The same absorbance in the O_2-free UV/VUV irradiated solution firstly increases and then very slowly decreases, which also confirms the importance of peroxyl radical in the transformation of intermediates.

5.1.3. Effect of pH

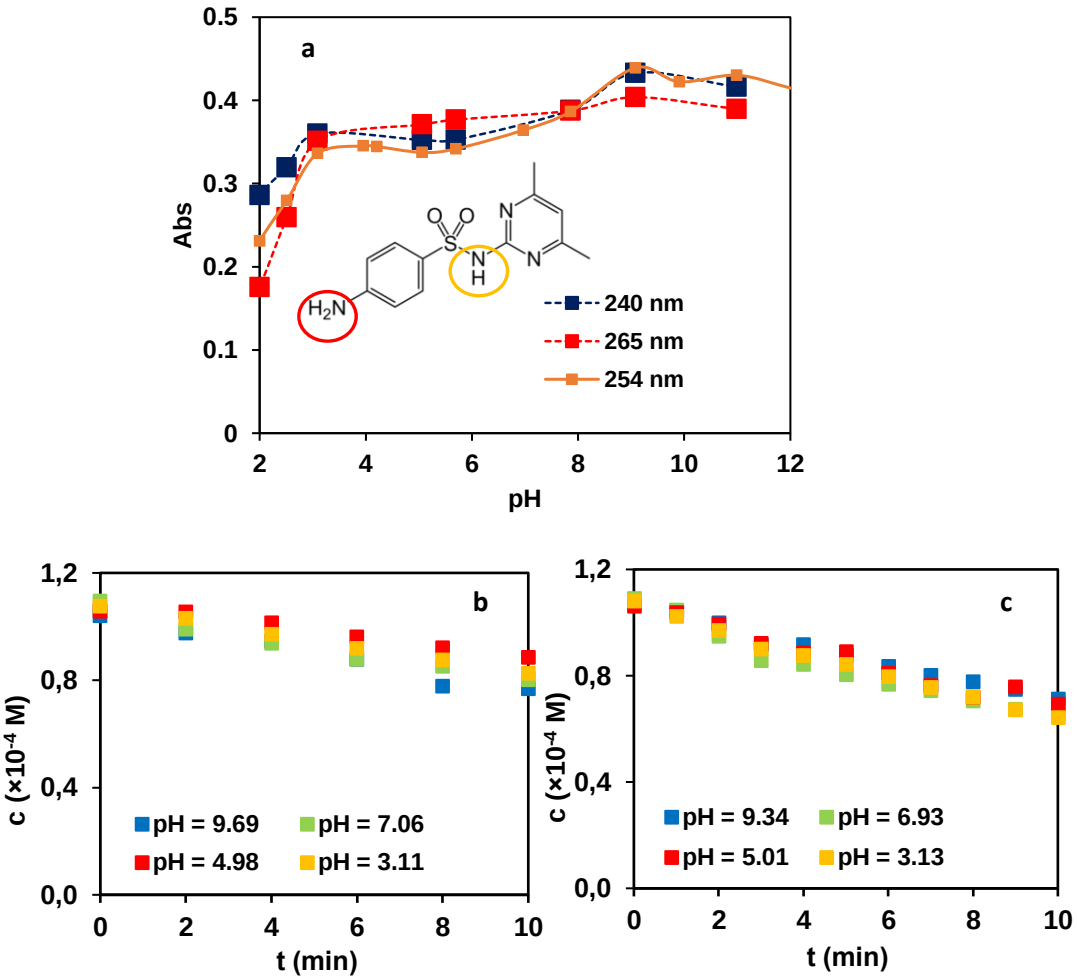

Figure 26. *Effect of pH on the absorbance at selected wavelengths (a) and the transformation rate of sulfamethazine in the case of UV (b) and UV/VUV photolysis (c)*

pH can affect the efficiency of UV photolysis by changing the absorbance and quantum yield of transformation, as reported by (Li et al., 2017). Both are strongly dependent on the degree of protonation of the compounds. Figures 26b and 26c show the transformation rates of SMT at various pH, while Figure 26a shows the absorbance determined at 240 and 265 nm (the characteristic peaks of SMT) and at 254 nm (the characteristic wavelength of the low-pressure mercury vapour lamp). Between pH 3 and pH 9 there is no significant effect of the pH on the absorbance (Figure 26a) and transformation rates (Figures 26b and 26c).

5.2. Ozonation and its combination with UV radiation (O_3/UV)

For the subsequent analysis of SMT transformation by ozonation and O_3/UV combination, and for the investigation of various matrices eventually, a new 4-points calibration has been used. Figures 27 and 28 show the spectra of the calibration solutions and the calibration curve, respectively.

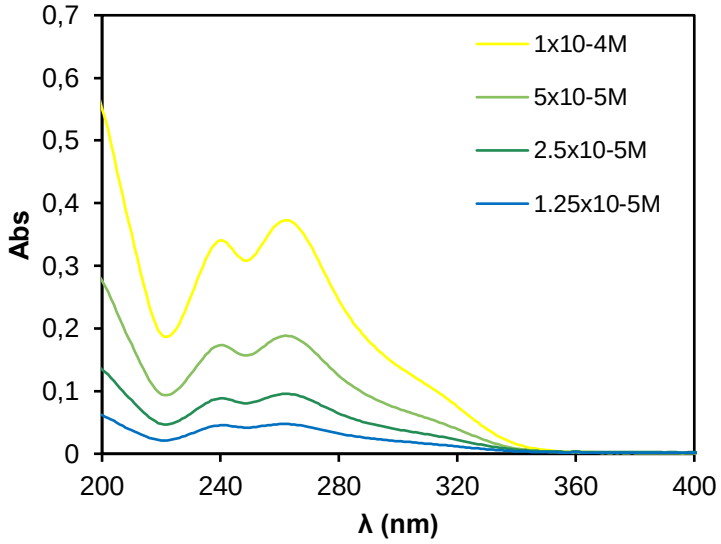

Figure 27. *Spectra of sulfamethazine in Milli-Q water*

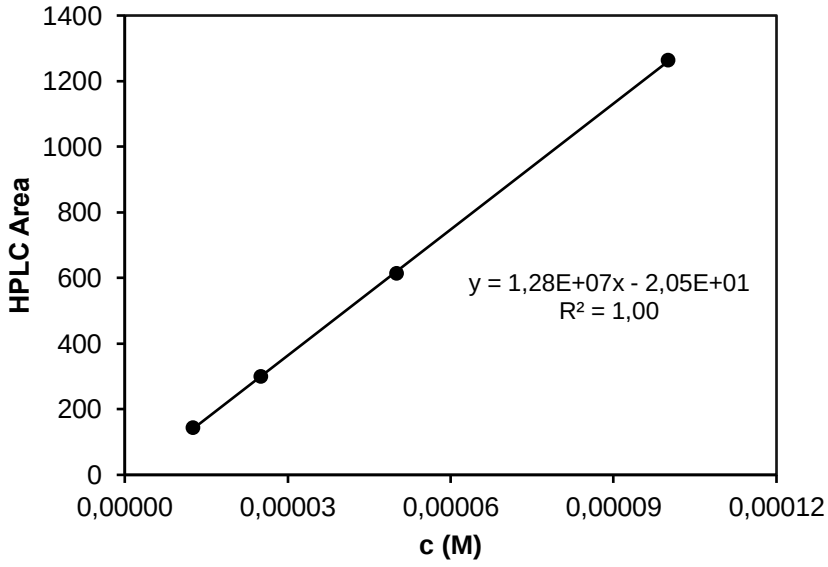

Figure 28. *Calibration curve of sulfamethazine measured with HPLC-DAD for ozonation and O_3/UV combination*

5.2.1. Transformation of sulfamethazine via ozonation and O_3/UV processes

The spectrum of O_3 has a maximum at 254 nm, and its molar absorbance in gas phase is $\varepsilon_{254\ nm} = 2950\ M^{-1}\ cm^{-1}$. The concentration of O_3 in gas phase was calculated according to the Lambert-Beer law (Figure 29).

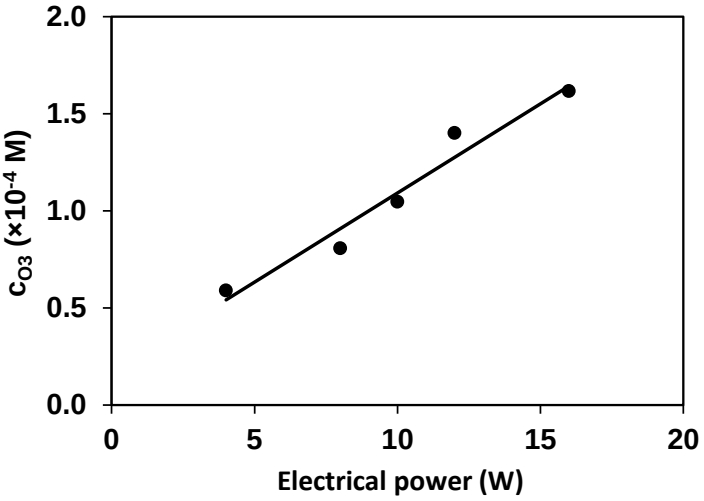

Figure 29. *Concentration of O_3 in gas phase versus the power of the Ozomatic Modular 4HC type ozonizator*

In the case of ozonation and its combination with UV light, the initial concentration of SMT was the same (1.0×10^{-4} M), the concentration of O_3 in gas phase (oxygen gas was used as feeding gas) was 1.3×10^{-4} M, and the dissolved O_3 concentration was two magnitude lower, 6.8×10^{-6} M. Ozonation was proved to be much more effective than UV or UV/VUV photolysis for the transformation of both SMT and its intermediates. The transformation of 90% of SMT requires 80 min in UV irradiated and 30 min in UV/VUV irradiated solutions. In the case of ozonation, this time was decreased to 7 min. Comparing the values of the initial transformation rates, those were more than two times higher in UV/VUV photolysis and almost one magnitude higher in the case of ozonation than in the case of UV radiation at 1.0×10^{-4} M initial concentration. Measurements were repeated at one magnitude lower of initial concentration of SMT (1.0×10^{-5} M). As shown in Table 9, the transformation rate was about forty times higher in the case of ozonation.

Table 9. *Initial transformation rate of sulfamethazine determined during ozonation and O_3/UV compared with UV and UV/VUV irradiated solution at various initial concentrations*

	c_0=1.0×10^{-4} M	c_0=1.0×10^{-5} M	c_0=1.0×10^{-4} M	c_0=1.0×10^{-5} M
	r_0 (×10^{-7} M s^{-1})		r_0/r_0^{UV}	
UV	0.32	0.03	–	–
UV/VUV	0.68	0.08	2.1	2.7
Ozonation	3.07	1.11	9.6	37
O_3/UV	3.20	1.29	10	43

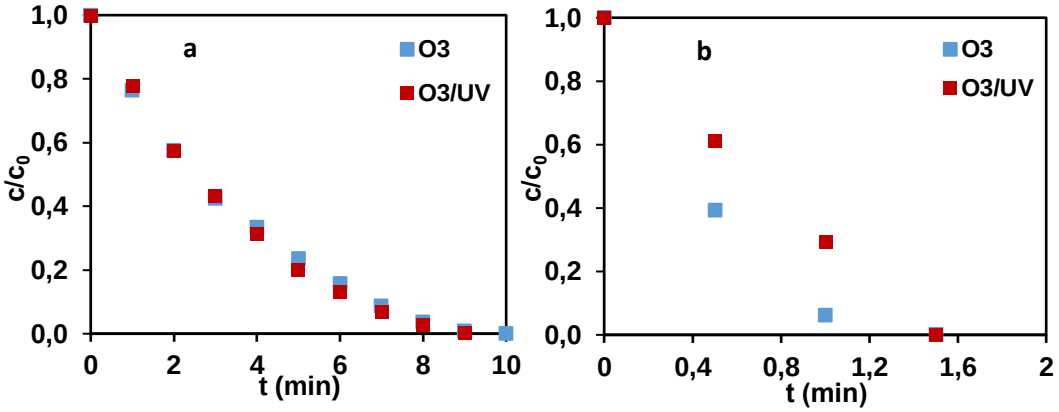

Figure 30. *Transformation of sulfamethazine in the case of ozonation and O_3/UV combination at 1.0×10^{-4} M (a) and at 1.0×10^{-5} M (b)*

When ozonation is used, there are various possibilities for the transformation of the organic substances: one of them is the direct reaction with O_3 molecule, and the other one is the reaction with •OH formed from O_3. Ozone is a quite selective oxidizing agent, the rate constant of its reaction with various organic substances changes between 10^{-4} and 10^9 M^{-1} s^{-1}, while •OH reacts with almost each substance close to the diffusion controlled transformation rate (10^9 M^{-1} s^{-1}). The formation rate of •OH from O_3 strongly depends on the pH of the solution, since it is a hydroxide-ion initiated chain reaction. The pH of the SMT solution was around 6.4 and decreased to 3.4 during the treatment. It is reasonable to suppose that, at this pH, SMT reacts mainly with molecular dissolved O_3 and •OH formation is negligible. The importance of ozone driven transformation was confirmed by the fact that, initial transformation rate cannot be influenced by the increase of pH to 3.0 or its decrease to 9.0. At pH 9.0, the relative high formation rate of •OH is expected. The negligible effect of pH decrease suggests similar values of the rate constants of SMT with O_3 and with •OH.

The significant difference between ozonation and UV photolysis becomes clear when the changes in spectra obtained during the two treatments are compared. The change of spectra in the presence of ozone (ozonation and its combination with UV photolysis) refers to the fast transformation of SMT and its intermediates having similar chemical

structure as SMT and probably similar reactivity toward O_3. If a comparison is made between the ozonation and its combination with UV photolysis, results showed no significant difference in either the initial transformation rate, the change in the shape of the spectrum, or the decrease in absorbance values between ozonation and the O_3/UV combination (Figure 30 and 31).

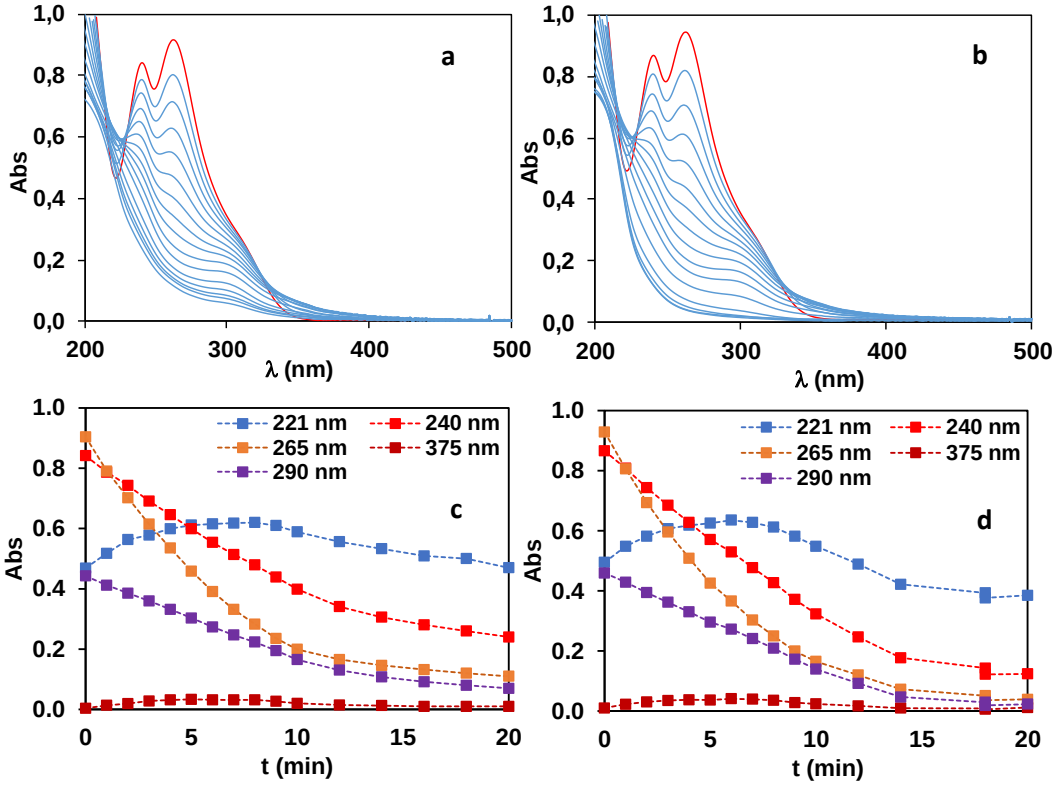

Figure 31. *Spectra of the treated solutions in the case of ozonation (a), O_3/UV combination (b) and the absorbance at some selected wavelengths (c: ozonation; d: O_3/UV combination)*

5.2.2. Effect of initial concentration of sulfamethazine and ozone

The transformation rate of SMT was very fast at relatively low ozone concentration. In this part of experimental work, the initial concentration of SMT was changed (in the range of 1.0×10^{-5} – 1.0×10^{-4} M) at constant ozone concentration ($c_{O3\ in\ gas\ phase}$ = 1.3×10^{-4} M). The concentration of dissolved O_3 changed between 6.8×10^{-6} and 3.5×10^{-5} M. In this case, the transformation rate of SMT increased linearly. In the subsequent step, the initial concentration of SMT was constant (1.0×10^{-4} M) and ozone concentration was changed between 1.3×10^{-4} and 3.0×10^{-4} M. The transformation rate increased linearly too (except at the highest value, determined at highest ozone concentration). Both observations

proved that the initial transformation rate of SMT can be described by the following equation in the presence of ozonation:

$$r_0 = k_{O3} \times [\text{sulfamethazine}] \times [O_3]$$

where r_0 is the initial transformation of SMT, k_{O3} is the rate constants of the reaction between SMT and dissolved ozone, [sulfamethazine] is the initial concentration of SMT and $[O_3]$ is the concentration of dissolved ozone.

In the case of the combination of ozonation with UV radiation, the initial transformation rate can be described by this way:

$$r_0 = k_{O3} \times [\text{sulfamethazine}] \times [O_3] + k_{\bullet OH} \times [\text{sulfamethazine}] \times [\bullet OH]$$

where [•OH] is the concentration of •OH, which depends on the concentration of dissolved ozone at constant photon flux (the transformation caused by direct UV photolysis of SMT was neglected in the presence of ozone). UV radiation did not enhance the transformation rate even at higher concentrations (Figure 32), which suggests that the value of the second member is much lower than that of the first one:

$$k_{\bullet OH} \times [\text{sulfamethazine}] \times [\bullet OH] << k_{O3} \times [\text{sulfamethazine}] \times [O_3]$$

At the same initial concentration of SMT, the following equation is valid:

$$k_{\bullet OH} \times [\bullet OH] << k_{O3} \times [O_3]$$

Most probably, the relative high value of k_{O3} and low concentration of •OH explain why the combination did not show better efficiency than simple ozonation.

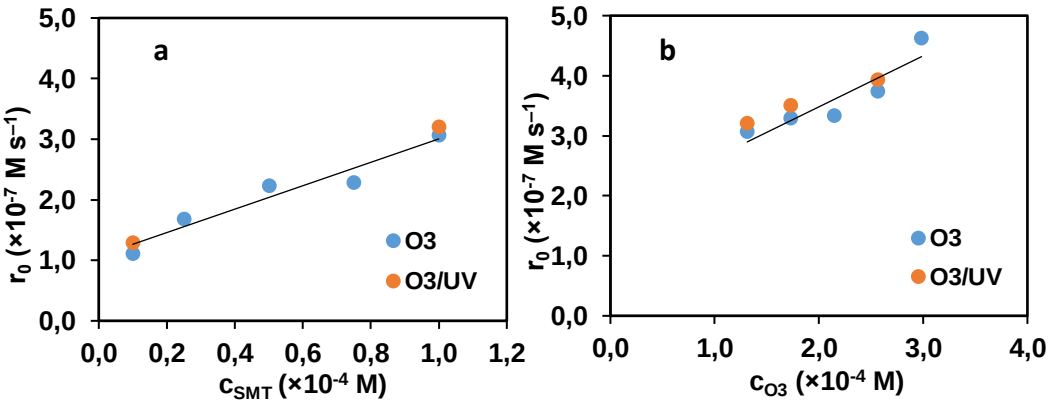

Figure 32. *Initial transformation rate at constant ozone concentration versus the initial concentration of sulfamethazine (a) and at constant sulfamethazine concentrations versus the ozone concentration in feeding gas (b)*

5.3. Investigation of the role of •OH

Both VUV photolysis of water and UV initiated transformation of O_3 produce highly reactive and nonselective •OH. In the case of the combination of ozonation with UV photolysis, the 254 nm photons initiate the formation of •OH; while in VUV irradiated solutions, •OH forms directly from water. The relative contribution of the •OH based reactions to the transformation of SMT was investigated via addition of terc-buthanol (TBA) as •OH scavenger. In the presence of a radical scavenger, competition occurs between SMT and TBA for •OH. Consequently, the transformation rate decreases. We have calculated the relative scavenging capacity ($RSC_{\bullet OH}$), which means the % of the •OH that reacts with TBA instead of with SMT. For this calculation, it is required to know the rate constants of TBA ($k_{TBA} = 6.0\times10^8$ M s^{-1} (Buxton et al., 1988)) and of SMT ($k_{SMT} = 8.3\times10^9$ M s^{-1} (Wojnárovits et al., 2018)) with •OH and their initial concentrations (c_{SMT} and c_{TBA}):

$$RSC_{\bullet OH} = \frac{c_{SM}\times k_{SM}}{c_{SM}\times k_{SM} + c_{TBA}\times k_{TBA}}\times 100$$

In UV/VUV radiated solution the decrease of the transformation rate depends on the initial concentration of TBA (1.5×10^{-4} M – 1.0×10^{-3} M). Close to the 100% $RSC_{\bullet OH}$, it decreases to the value determined in UV radiated solution (Figure 33). This clearly proves that the relative contribution of the •OH based reaction is similar to that of the direct UV photolysis. It is worth to mention here again that, the intensity of VUV light is one magnitude lower than that of UV light.

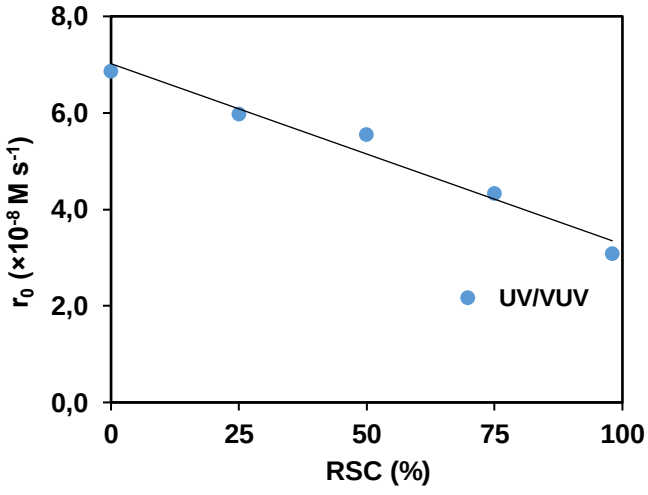

Figure 33. *Initial transformation rate of sulfamethazine versus the relative scavenging capacity using TBA as •OH scavenger*

In the case of ozonation and its combination with UV light, in order to investigate the role of •OH, it was used that concentration of TBA when 98% of the •OH reacts with TBA instead of SMT. The effect of TBA was negligible in the case of both processes (Figure 34). This result underlined that, in the case of ozonation and its combination with UV photolysis, the relative contribution of •OH initiated transformation of SMT is negligible besides its reaction with ozone. Nevertheless, this does not mean that there is no •OH formation in the UV irradiated O_3 containing solutions.

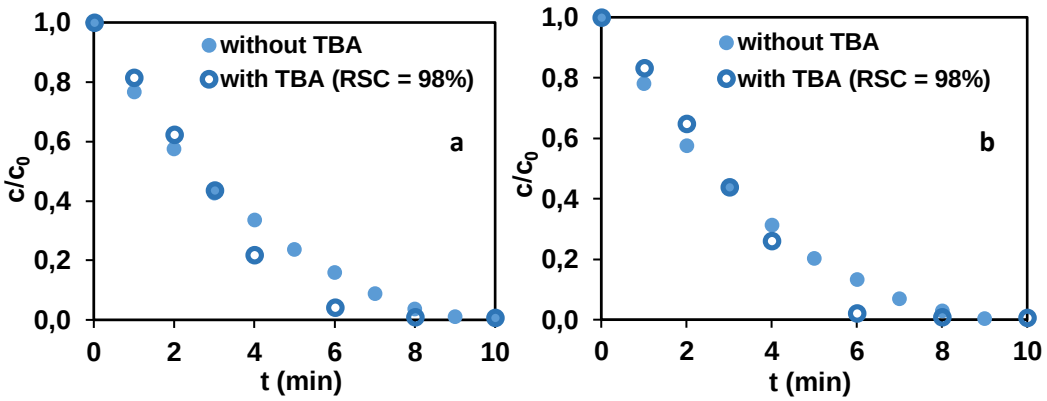

Figure 34. *Effect of TBA on the transformation rate of sulfamethazine in the case of ozonation (a) and UV/O_3 process (b)*

5.4. Intermediates

The identification of the intermediates formed during the treatments was provided by HPLC-MS method after SPE sample pre-treatment. The *m/z* values of the detected intermediates are presented in Table 10. In the case of each process, hydroxylated products (*m/z* = 293.1) were detected although in UV radiated solution there is no •OH transformation and in the presence of ozone the relative contribution of •OH based reaction to the transformation is not probable. The different retention times, but same *m/z* value of hydroxylated products, suggests that various isomers can form via hydroxylation. The formation of hydroxylated intermediates was published also by several authors (Li et al., 2017; Nassar et al., 2017; Zhu et al., 2019). It is noteworthy that the transformation of aromatic organic substances is often accompanied by the formation of hydroxylated products even in the case of direct UV photolysis and ozonation. Thus, their presence in the treated solution did not prove the role of •OH in the transformation.

Table 10. *m/z values of sulfamethazine and its intermediates*

	UV/VUV aerated	UV/VUV O_2-free	UV aerated	UV O_2-free	O_3	O_3/UV
t_r (min)	m/z	m/z	m/z	m/z	m/z	m/z
1.60		291.0			285.0	285.0
1.69		293.1				
1.81		275.0		293.1	321.0	307.0
2.01					323.0	323.0
2.12		294.7				
2.21				293.1		323.0
2.32					323.0	
2.46		293.1				
2.52				293.0		
2.87						341.0
3.21		383.9				
3.38				303.9		
3.53	291.0		291.0		291.0	291.0
3.88					244.0	
4.99	309.0					
5.45	293.1	293.1			293.1	
5.54						356.0
5.76	294.7					
6.67	277.1 SMT	277.1	277.1	277.1	277.1	277.1
9.33	293.1					

Applying O_3/UV process, the methyl moiety (-CH_3) can transform into carboxyl group (-COOH; *m/z* = 307.0). The amino moiety (-NH_2) of SMT is able to transform to nitroso moiety (-NO; *m/z* = 291.0). This reaction pathway was proved by Zhu et al. (2019). In the case of UV/VUV photolysis, besides hydroxylation, the amino moiety transforms to nitro-group (-NO_2; *m/z* = 323.0), probably via •OH initiated reaction. This intermediate is suggested by Liu et al. (2018). Identified intermediates are shown in Figure 35.

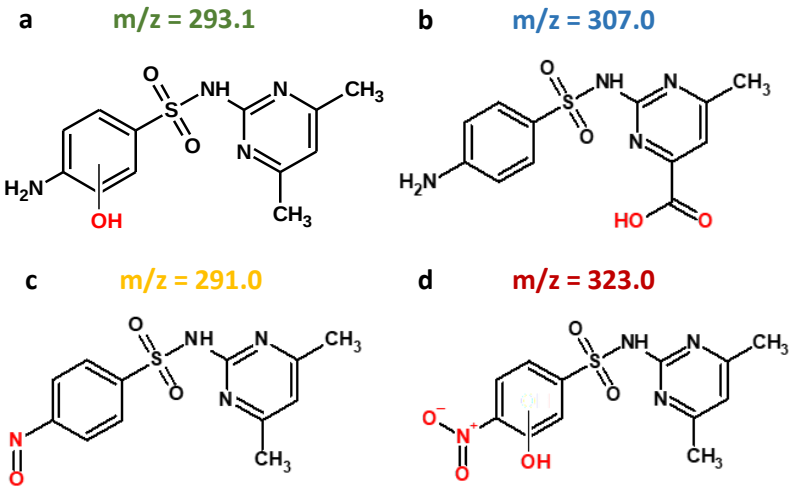

Figure 35. *Chemical structure of the identified intermediates formed from sulfamethazine*

5.5 Mineralization

When the elimination of toxic or harmful organic substances is the goal of a process, generally the investigation of the transformation of a target substance is not enough, because the formed intermediates may also include biologically active compounds. Consequently, the goal is both to transform and mineralize the target pollutant.

The methods efficiency was characterized via decrease of the Chemical Oxygen Demand (COD) and Total Organic Carbon concentration (TOC). However, when 1.0×10^{-4} M SMT transformed within 120 minutes (Figure 24), there was no change of COD and TOC in UV radiated aerated solution during this time (Figure 36).

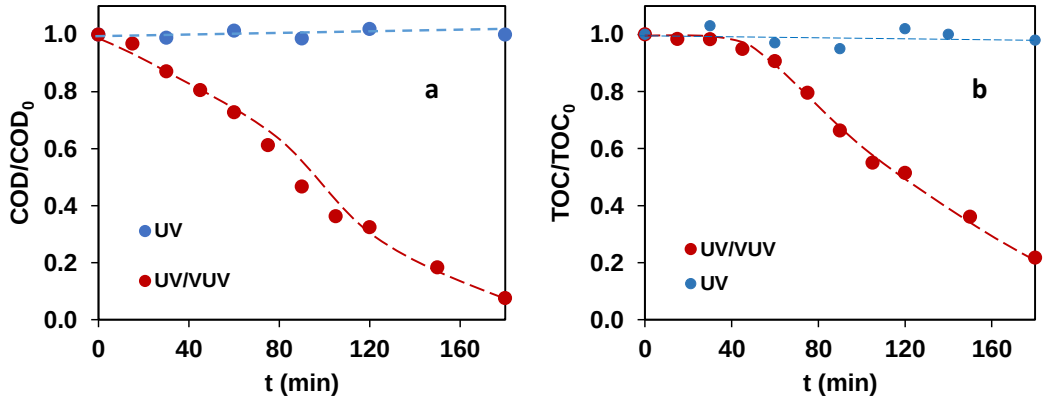

Figure 36. *Decrease of COD (a) and TOC (b) values in UV and UV/VUV radiated aerated solutions*

In UV/VUV irradiated solution, 1.0×10^{-4} M SMT transformed in 60 minutes (Figure 25). During this time there was no significant change of TOC, but COD decreased linearly by 28% (Figure 36). After this first period, both COD and TOC decreased intensively and only 8% of COD and 22% of TOC remained in the solution after 3-hours treatment. This is in line with previous conclusions that •OH formed due to low intensity VUV significantly increases the transformation rate of SMT and of its intermediates.

Ozonation was much more effective for SMT elimination than photolysis. In the case of ozonation, COD decreased intensively during the transformation of SMT. COD deceased was almost 40% within 10 minutes, while TOC decreased by less than 10% (Figure 37). Independently on the ozone concentration, the TOC value decreased by less than 20%, while COD decrease did not exceed 50% after 30 min treatment. Both TOC and COD values became constant eventually (Figure 37). The observation can be explained by the fast reaction of ozone with SMT and some intermediates probably having a similar chemical structure as SMT, whose processes are associated with a reduction in TOC and COD. It

should be kept in mind that ozone is a very selective oxidizing agent and several intermediates can form, which might be resistant towards reaction with molecular ozone. Thus, after the transformation of substances, which are highly reactive towards ozone, several intermediates may remain in the solutions without reacting or very slowly reacting with ozone.

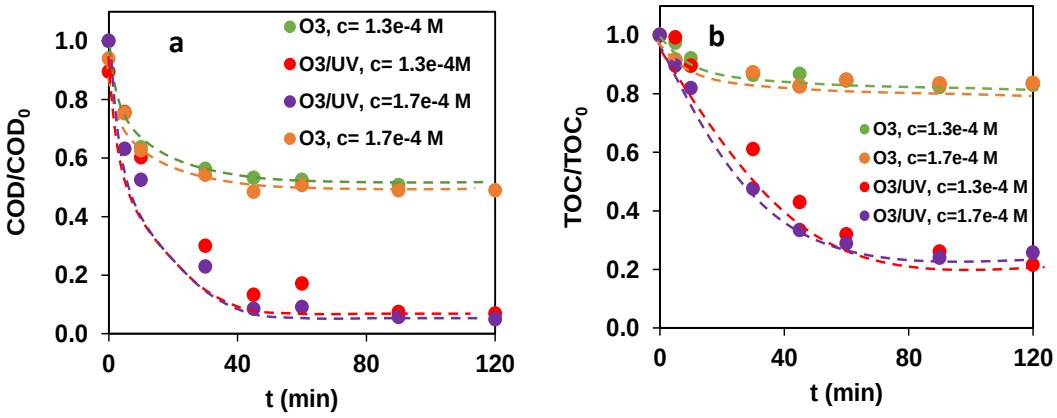

Figure 37. *Decrease of COD (a) and TOC (b) values in the case of ozonation and O_3/UV process at two different ozone concentrations*

Although UV radiation does not enhance the transformation rate of SMT, it has a significant positive effect on the mineralization. The combined presence of ozone and 254 nm radiation caused 90% decrease of COD and 80% of TOC within 60 min. In this case, intermediates, which are not reactive towards ozone, can be decomposed easily via •OH based reactions. At the same time, the increase of ozone concentration has no effect on the mineralization efficiency (Figure 37).

The transformation of organic substances is accompanied by the formation of peroxyl radicals. The further transformation of peroxyl radical generally results in accumulation of HO_2• and O_2•$^-$. As reported in introduction, these radicals have low reactivity and their role in the transformation of organic substances is negligible. Instead of the reaction with organic molecules, their recombination takes place and finally results in the formation of H_2O_2. Thus, the change in the concentration of H_2O_2 indicates the intensity of oxidative conversion of organic matter and it is related to the change in COD and TOC.

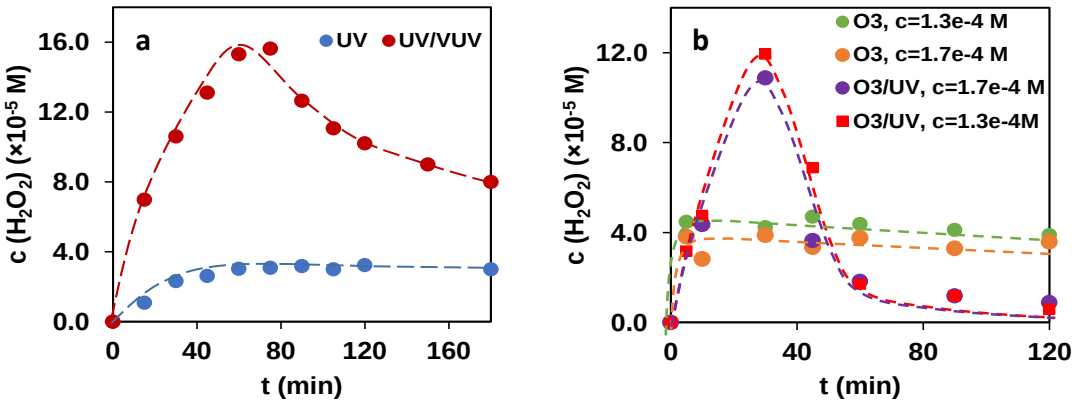

Figure 38. *H_2O_2 concentration in UV and UV/VUV radiated solutions (a) and in the case of ozonation and O_3/UV process (b) at two different ozone concentrations*

Although the change in TOC and COD was negligible during UV treatment (Figure 36), the transformation of SMT (Figure 24) was associated with some H_2O_2 formation (Figure 38). In this case, only the slow accumulation of H_2O_2 was observed. On the other hand, applying UV/VUV process, an intensive H_2O_2 accumulation and its slower transformation take place. The H_2O_2 concentration reaches its maxima at 60 min treatment, when COD and TOC decrease became faster. After 120 minutes both mineralization rate and H_2O_2 concentration decrease are slowed down slightly (Figure 37 and 38a).

During ozonation, after a sudden increase, the H_2O_2 concentration became practically constant (Figure 38b). The short (10 min) first period is characterized by a rapid conversion of SMT and a concomitant intense decrease in COD and TOC (Figure 37). All of these suggest an extremely rapid and efficient oxidation of the starting material and of some intermediates. After this time, the H_2O_2 concentration remains practically constant, in line with the fact that both COD and TOC values do not change after 60 minutes (Figure 37 and 38b). All these considerations confirm the assumption that intermediates are formed during ozonation, but they cannot be efficiently converted by this process.

When ozonation is combined with UV radiation, H_2O_2 concentration changed according to the maximum curve (Figure 38b): its intensive increase and decrease takes place together with the rapid decrease in COD and TOC values (Figure 37).

NO_3^- ions were measured during UV/VUV photolysis in order to get further information on the mineralization and the possible elimination of the nitro groups from SMT. The UV/VUV sampling revealed a slight absorbance at 350 nm. It means that only a small amount of NO_3^- was in solution, probably due to the presence of reducing agents (*i.e.*, H• and e_{aq}^-) produced from VUV photolysis of water (Li et al., 2017). The strong overlap of the spectra at 350 nm between NO_3^- and SMT could be another reason for the inability to

determine the NO_3^- concentration. Since the NO_3^- concentration detected was low, the UV sampling was not carried out considering that the degradation rate would have been even lower in the same reaction time.

5.6 Ecotoxicity measurements

During the oxidative transformation of a contaminant, not only its transformation, but also the change in the toxicity of the resulting multicomponent mixture is a very important issue. The change of the ecotoxicity of the treated solutions with various processes was followed via inhibition of the luminescent light emitted by the *Vibrio fischeri* test organism.

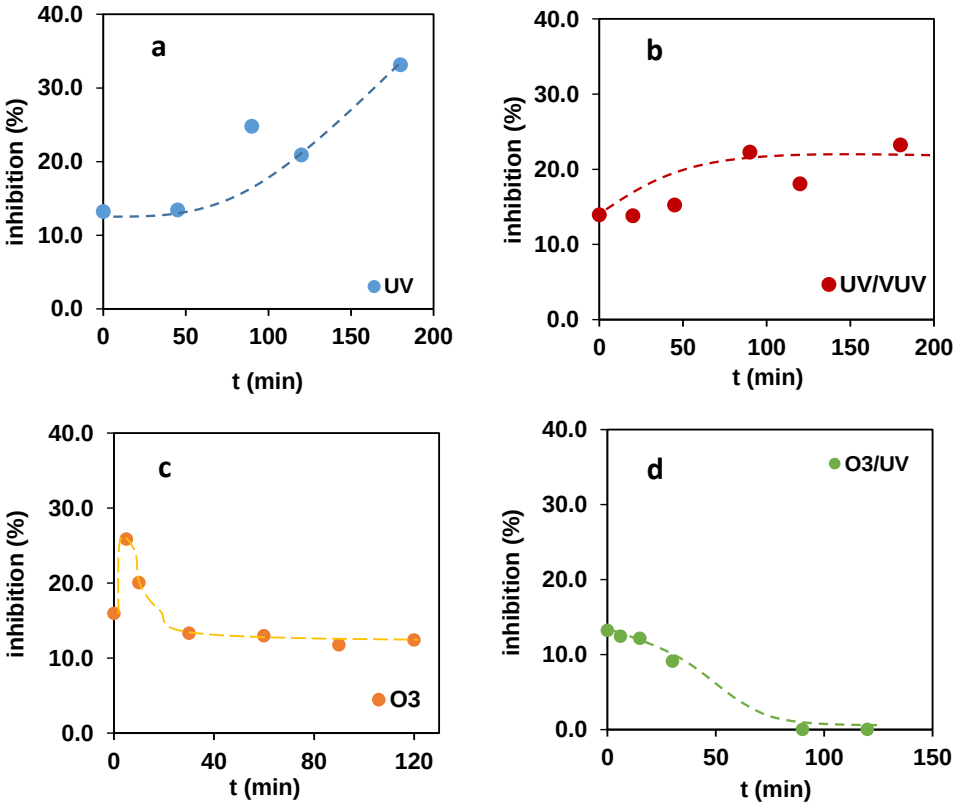

Figure 39. *Inhibition effect of the treated solutions versus the time of treatment during UV photolysis (a), UV/VUV photolysis (b), ozonation (c) and O_3/UV combination (d)*

In the case of UV photolysis, ecotoxicity increased (Figure 39a) probably because of the accumulation of various aromatic intermediates. Using UV/VUV photolysis, inhibition effect increased at the beginning and then it became constant (Figure 39b). When ozonation was applied, the ecotoxicity increased and reached a maximum when SMT was

completely transformed. Its decrease refers to the transformation of some intermediates, but later it became constant (Figure 39c) due to the formation of stable intermediates (Figures 37 and 38b), which do not react with ozone. The most effective treatment for ecotoxicity decrease was the O_3/UV process. By the end of the treatment (approximately 80 min), the ecotoxicity was completely absent (Figure 39d).

5.6. Effect of various matrices

From the point of view of the application on various water treatment processes, the effect of matrix on the efficiency is crucial. Since the applied processes can be used as post-treatment or tertiary treatment, two mild matrices were used: tap water from Szeged and biologically treated wastewater. Table 5 presents the analytical data of applied matrices, while Table 11 contains the reaction rates of SMT transformation determined in these matrices.

In the case of UV photolysis any matrix can behave as a "filter", decreasing the efficiency via absorption of 254 nm UV light. In our cases, absorbance of both matrices was negligible at 254 nm (Figure 40). The presence of various organic and inorganic component is able to decrease the efficiency via reaction with reactive species (ozone or •OH). At the same time, some components can cause higher transformation rate via photosensitization or enhancing the transformation of ozone as promotor.

Table 11. *Effect of various matrices on the initial transformation rate*

c_0 (M)		r_0 ($\times 10^{-7}$ M s^{-1})		
		MQ	**Tap water**	**Purified wastewater**
1.0×10^{-4} M	**UV**	0.32	0.42	0.45
	UV/VUV	0.68	0.74	0.88
	Ozonation	2.01	2.65	3.41
	O_3/UV	2.16	3.04	3.81

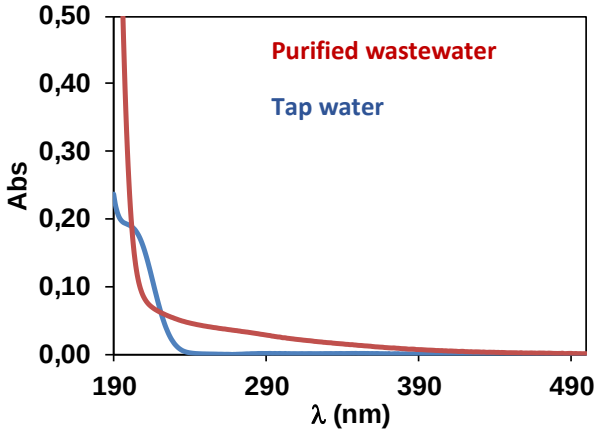

Figure 40. *Absorbance of the matrices*

It has been demonstrated that both matrices slightly enhanced the transformation rate. In the case of tap water, the results can be explained by the UV photolysis of HOCl, which can produce in the formation of both •Cl and •OH:

$HOCl + h\nu \rightarrow$ •OH + •Cl $1.45 < \phi = 240\text{-}365 \text{ nm} < 1.64$ (Wang et al., 2012)

•Cl + HOCl $\rightarrow Cl_2$ + •OH (Kukui et al., 1997)

The confirmation of the role played by these reactions needs further experimental work and investigation.

5.7. Electric Energy per Order (E_{EO})

Electrical Energy per Order (E_{EO}) represents the amount of electric energy required for reduction of the target compound concentration in a unit volume (*i.e.*, 1 m^3) by one order of magnitude. Using the model developed by James Bolton, E_{EO} can be calculated from the electrical power required for ozone production and/or for operating the light source. The time required for the transformation of 90% of 1.0×10^{-4} M SMT was determined from the kinetic curve of its transformation.

Based on the comparison of the values, ozone treatment is clearly the most cost-effective method together with the O_3/UV combination (Figure 41).

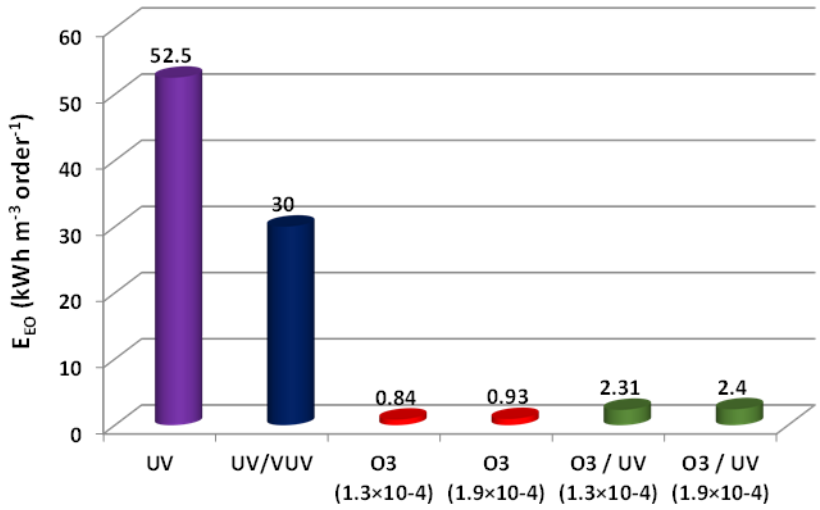

Figure 41. *Electrical energy requirement of the various processes for transformation of 90% of sulfamethazine at 1.0×10^{-4} M initial concentration*

However, it is worth considering that this efficiency by itself is not sufficient to state that ozonation is the best treatment for SMT removal. In fact, it was shown that in the treated solution contains several non-ozone-reactive intermediates, the exact biological effects are unknown. The ecotoxicity of the resulting multicomponent solution after ozonation is comparable to that of the starting SMT solution.

6. Conclusions

It has been proved that the most efficient method to decompose sulfamethazine (SMT) in aqueous solutions (c_0 = 1.0×10^{-4} and 1.0×10^{-5} M) among the tested treatments was simple ozonation. The reason is the high reaction rate of SMT towards molecular ozone. The combination O_3/UV had no significant additional effect on the transformation of SMT; however, enhanced •OH formation rate due to the UV initiated transformation of O_3 had an important role in the mineralization of the degradation products.

UV/VUV photolysis was more efficient for the transformation and mineralization of SMT than simple UV photolysis due to additional effect of •OH formed from water. Although dissolved O_2 had no significant effect on the transformation rate of SMT during UV/VUV photolysis, its presence highly effected the change of the spectrum probably due to the joint effect of •OH and O_2. It was interesting to observe the absorbance in the spectra at 221 nm: while during UV photolysis it increased throughout the duration of UV radiation, in UV/VUV, after a slight increase, an intense decrease was observed, meaning that the transformation of intermediates is more efficient during UV/VUV photolysis.

According to the role of terc-buthanol (TBA) as •OH scavenger, the relative contribution of •OH initiated reactions to the transformation of SMT was negligible in the case of simple ozonation and O_3/UV process, while it was proved to be significant in UV/VUV radiated solution.

Besides considering the effectiveness of the degradation of the target compound, the mineralization of the SMT should be also considered. During simple ozonation, after a fast reduction of the TOC and COD values, no more than 20% of TOC and 40% of COD was removed. The combined presence of ozone and UV radiation caused 90% decrease of COD and 80% of TOC after 60 min treatment. In this latter case, intermediates, which are not reactive towards ozone, can be decomposed easily via •OH based reactions. Moreover, increase of ozone concentration had no effect on the mineralization efficiency. No change of COD and TOC was measured during UV photolysis in 120 min irradiation time, while in UV/VUV irradiated solution only 8% of COD and 22% of TOC remained in the solution after 3-hours treatment. The trend of H_2O_2 concentration change was consistent with these results in the case of each method.

Ecotoxicological tests on *V. fischeri* found that, at the end of simple ozonation, several non-ozone-reactive intermediates were still present in the treated solution, causing toxic effects on the tested organisms. The exact biological effects of these intermediates are

however unknown. On the other hand, O_3/UV process was proved to be the most effective method for ecotoxicity decrease, reducing completely the hazard approximately in 80 min. Regarding UV and UV/VUV photolysis, ecotoxicity results showed an increase in the toxic potential of the treated solutions, probably because of the accumulation of various aromatic intermediates.

The detection of four intermediates of SMT was possible by using HPLC-MS. For each process, various hydroxylated isomeric products were detected and two out four of them were in common with every method (*m/z* = 291.0, 293.1).

The calculation of the Electric Energy per Order value allowed to get information about the economic aspect of the treatments in terms of electric energy consumption. Ozone treatment (0.84 kWh m^{-3} $order^{-1}$) was found to be the most cost-effective method together with the O_3/UV combination (2.31 kWh m^{-3} $order^{-1}$), followed by UV/VUV photolysis (30 kWh m^{-3} $order^{-1}$) and then UV photolysis (52.5 kWh m^{-3} $order^{-1}$). This aspect is very important in order to find out the best solution in terms of economic factor for a possible future large-scale water treatment plant. Relating to a real-scale application, the importance of testing the effect of different matrices on the degradation of SMT is crucial. The two mild matrices tested (tap water and treated wastewater) have shown a slightly enhancement on the transformation rate of the target compound; especially in tap water, possibly because the presence of HOCl resulted in the formation of further reactive radicals such as •Cl and •OH.

In the future more studies are required in order to get deeper information about the effect of different matrices as well as transformation products formed under different AOP technologies. Moreover, it would be interesting to perform further ecotoxicological tests to get to know better the exact biological effects of SMT and of its degradation products.

7. Acknowledgements

This thesis has been developed at the Department of Inorganic and Analytical Chemistry of the University of Szeged. Szeged is a city in the south of Hungary which hosted me as a student for the Erasmus+ *for traineeships* program from February until the end of July 2019. I had the pleasure of working in the central square of the city, in front of the Dom of Szeged, together with the research group of Environmental Chemistry. I would like to say thank you once again to Dr. Tünde Alapi, for giving me the opportunity to collaborate with them and for making me feel welcome, and to PhD students Luca Farkas and Máté Náfrádi for all the good advises during my experience in the laboratory. Köszönöm!

I would also like to thank you to my supervisor, Prof. Valerio Di Marco from the Department of Chemistry at the University of Padova for suggesting me this country and its people, and for the support during the whole experience abroad as well as during the writing time of the thesis. He always shows great humanity and availability for students.

My life in Szeged was unforgettable. I have met dozens of international students and my flatmates were great. I have spent wonderful moments with them, organising also some excursion around Hungary to discover other places and to know the Hungarian culture better. Thanks to them, I was never alone. It was so surprising to see international students sharing thoughts and memories with everybody. This experience made me grow up as a person and contributed to solidify my personality.

Last but not least, I need to say thanks to my family, for their endless support and for teaching me to believe in myself.

A great thank you to all my “Italian friends”, you are surely the craziest and most special people I could have ever ask for.

I am going to write down these last words conscious that this is just the end of incredible chapter and that other great experiences are yet to come.

7. Ringraziamenti

Questa tesi è stata svolta al Dipartimento di Chimica Inorganica e Analitica dell'Università di Szeged. Szeged è una città nel sud dell'Ungheria che mi ha accolto come studentessa per il programma Erasmus+ *for traineeships* da febbraio fino alla fine di luglio 2019. Ho avuto il piacere di lavorare nella piazza centrale della città, di fronte al Duomo di Szeged, insieme al gruppo di ricerca di Chimica Ambientale. Vorrei ringraziare ancora una volta la Dott.ssa Tünde Alapi, per avermi dato l'opportunità di collaborare con loro e per avermi fatto sentire la benvenuta, e i dottorandi Luca Farkas e Máté Náfrádi per tutti i consigli durante la mia esperienza in laboratorio. Köszönöm!

Vorrei anche ringraziare il mio supervisore, il Prof. Valerio Di Marco del Dipartimento di Chimica dell'Università di Padova per avermi suggerito questo paese e i suoi abitanti, e per il supporto durante l'intera esperienza all'estero oltre che durante la stesura della tesi. Ha sempre mostrato una grande umanità e disponibilità nei confronti degli studenti.

La mia vita a Szeged è stata indimenticabile. Ho incontrato decine di studenti internazionali e le mie coinquiline erano fantastiche. Ho vissuto meravigliosi momenti con loro, organizzando anche delle uscite nel resto dell'Ungheria in modo da scoprire altri posti e conoscere meglio la cultura ungherese. Grazie a loro, non mi sono mai sentita da sola. È stato sorprendente vedere studenti provenienti da tutto il mondo condividere pensieri e ricordi con tutti. Questa esperienza mi ha fatto crescere come persona e ha contribuito a solidificare la mia personalità.

Ultimo ma non per importanza, è doveroso ringraziare la mia famiglia, per il loro illimitato supporto e per avermi insegnato a credere in me stessa.

Un grande saluto va anche a tutti i miei "amici italiani", siete di sicuro le persone più pazze e speciali che avrei mai potuto incontrare.

Sto per scrivere queste ultime parole con la consapevolezza che questa è solo la fine di un incredibile capitolo e che altre fantastiche esperienze ci saranno.

8. Appendix

ECs	Emerging Contaminants
PPCPs	Pharmaceutical and Personal Care Products
LOD	Limit of Detection
LOQ	Limit of Quantification
WWTP	Wastewater Treatment Plant
AOPs	Advanced Oxidation Processes
UV	Ultraviolet
VUV	Vacuum Ultraviolet
•OH	Hydroxyl radical
H•	Hydrogen radical
e^-_{aq}	Hydrated Electron
LPM lamp	Low Pressure Mercury lamp
E_{EO}	Electrical Energy per Order
TOC	Total Organic Carbon
COD	Chemical Oxygen Demand
H_2O_2	Hydrogen Peroxide
VABs	Veterinary Antibiotics
AMR	Antimicrobial Resistance
POPs	Persistent Organic Pollutants
PABA	*p*-aminobenzoic acid
SMT	Sulfamethazine
MeOH	Methanol
HCOOH	Formic Acid
TBA	Terc-buthanol
RSC	Relative Scavenging Capacity
HPLC	High Pressure Liquid Chromatography
DAD	Diode Array Detector
ESI	Electrospray Ionization
MS	Mass Spectrometry
t_r	Retention time
m/z	Mass to charge
SPE	Solid Phase Extraction

9. References

Aarestrup F. Sustainable farming: Get pigs off antibiotics. Nature, 2012 Jun; 486(7404): 465-466.

Adams C.; Asce M.; Wang Y.; Loftin K.; Meyer M. Removal of Antibiotics from Surface and Distilled Water in Conventional Water Treatment Processes. Journal of Environmental Engineering. 2002 Mar; 128(3): 253-260.

Alapi T. and Dombi A. Comparative study of the UV and UV/VUV-induced photolysis of phenol in aqueous solution. Journal of Photochemistry and Photobiology A: Chemistry. 2007 May; 188(2-3): 409-418.

Alvares A. B., Diaper C. and A. Parsons S. Partial Oxidation by Ozone to Remove Recalcitrance from Wastewaters: a Review. Environmental Technology. 2001 Apr; 22(4): 409-427.

Amor C.; Marchão L.; Lucas M. S.; Peres J. A. Application of Advanced Oxidation Processes for the Treatment of Recalcitrant Agro-Industrial Wastewater: A Review. Water. 2019 Jan; 11(2): 205.

Andreozzi R.; Caprio V.; Insola A.; Marotta R. Advanced oxidation processes (AOP) for water purification and recovery. Catalysis Today. 1999 Oct; 53(1): 51-59.

Babić S.; Zrnčić M.; Ljubas D.; Ćurković L.; Škorić I. Photolytic and thin TiO_2 film assisted photocatalytic degradation of sulfamethazine in aqueous solution. Environmental Science and Pollution Research. 2015; 22(15): 11372–11386.

Banerjee S. and Mazumdar S. Electrospray Ionization Mass Spectrometry: A Technique to Access the Information beyond the Molecular Weight of the Analyte. International Journal of Analytical Chemistry. 2012: 282574.

Baran W.; Adamek E.; Ziemianska J.; Sobczak A. Baran W. Effects of the presence of sulfonamides in the environment and their influence on human health. Journal of Hazardous Materials. 2011 Nov; 196(30): 1-15.

Battista A. P. S., Pires F. C. C. and Teixeira A. C. S. C. Photochemical degradation of sulfadiazine, sulfamerazine and sulfamethazine: Relevance of concentration and heterocyclic aromatic groups to degradation kinetics. Journal of Photochemistry and Photobiology A: Chemistry, 2014; 286: 40-46.

Ben W.; Qiang Z.; Pan X.; Nie Y. Degradation of veterinary antibiotics by ozone in swine wastewater pretreated with sequencing batch reactor. Journal of Environment and Engineering. 2012 Mar; 138(3): 272-277.

Bielski B. H. J.; Cabelli D. E.; Arudi R.L.; Ross A. B. Reactivity of HO_2/O^-_2 radicals in aqueous solution. Journal of Physical and Chemical Reference Data 14. 1985; 1041–1100.

Binh V. N.; Dang N.; Anh N. T. K.; Ky L. K.; Thai P. K. Antibiotics in the aquatic environment of Vietnam: Sources, concentrations, risk and control strategy. Chemosphere. 2018 Apr; 197: 438-450.

Biošić M., Mitrevski M. and Babić S. Environmental behavior of sulfadiazine, sulfamethazine,and their metabolites. Environmental Science and Pollution Research International. 2017 Apr; 24(10): 9802-9812.

Bolto J. R.; Bircher K. G.; Tumas W.; Tolman C. A. Figure-of-merit for the technical development and application of advanced oxidation technologies for both electric- and solar-driven systems. Pure and Applied Chemistry. 2001 Dec; 73(4): 627-637.

Boreen A. L., Arnold W. A. and McNell K. Triplet-Sensitized Photodegradation of Sulfa Drugs Containing Six-Membered Heretocyclic Groups: Identification of an SO2 Extrusion Photoproduct. Environmental Science & Technology. 2005 May; 39(10): 3630-3638.

Brain R. A.; Johnson D. J.; Richards S. M.; Sanderson S.; Sibley P. K.; Solomon K. R. Effects of 25 pharmaceutical compounds to Lemnia gibba using a seven-day static-renewal test. Environmental Toxicology and Chemistry. 2004 Feb; 23(2): 371–382.

Braun A. M., Maurette M. T. and Oliveros E. Photochemical Technology. Chichester: John Wiley & Sons. 1991.

Buxton G. V.; Greenstock C. L.; Helman V. P.; Ross A. B. Critical Review of rate constants for reactions of hydrated electrons, hydrogen atoms and hydroxyl radicals (•OH/•O^-) in aqueous solution. Journal of Physical and Chemical Reference Data 17. 1988; 513.

Carvalho I. T. and Santos S. Antibiotics in the aquatic environments: A review of the European scenario. Environment International. 2016 Sep; 94: 736-757.

Chua B.; Goyne K. W.; Anderson S. H.; Lin C. H.; Lerch R. N. Sulfamethazine Sorption to Soil: Vegetative Management, pH, and Dissolved Organic Matter Effects. Journal of Environmental Quality. 2013 May-Jun; 42(3): 794-805.

Conde-Cid M.; Fernández-Calviño D.; Nóvoa-Muñoz J. C.; Arias-Estévez M.; Díaz-Raviña M.; Núñez-Delgado A.; Fernández-Sanjurjo M. J.; Álvarez-Rodríguez E. Degradation of sulfadiazine, sulfachloropyridazine and sulfamethazine in aqueous media. Journal of Environmental Management. 2018 Dec; 228: 239-248.

Conde-Cid M.; Alvarez-Esmorísa C.; Paradelo-Núnez R.; Novoa-Munoz J. C.; Arias-Estevez M.; Alvarez-Rodríguez E.; Fernandez-Sanjurjo M. J.; Núnez-Delgado A. Occurrence of tetracyclines and sulfonamides in manures, agriculturalsoils and crops from different areas in Galicia (NW Spain). Journal of Cleaner Production. 2018 Jun; 197: 491-500.

Cuerda-Correa E. M., Alexandre-Franco M. F. and Fernández-González C. Advanced Oxidation Processes for the Removal of Antibiotics from Water. An Overview. Water. 2019 Dec; 12(102).

Deng Y. and Zhao R. Advanced Oxidation Processes (AOPs) in Wastewater Treatment. Current Pollution Reports. 2015 Sep; 1(3): 167-176.

Dolliver H., Kumar K. and Gupta S. Sulfamethazine Uptake by Plants from Manure-Amended Soil. Journal of Environmental Quality. 2007 Jul; 36(4): 1224-1230.

Du L. and Liu W. Occurrence, fate, and ecotoxicity of antibiotics in agro-ecosystems. A review. Agronomy for Sustainable Development. 2012 Jan; 32(2): 309-327.

Council Regulation (EEC) No 2377/90 of 26 June 1990 laying down a Community procedure for the establishment of maximum residue limits of veterinary medicinal products in foodstuffs of animal origin.

Eliasson B. and Kogelschatz U. UV Excimer Radiation from Dielectric-Barrier Discharges. Applied Physics B. 1988 Aug; 46: 299-303.

European Centre for Disease Prevention and Control. Surveillance of antimicrobial resistance in Europe 2018. Stockholm : ECDC, 2019.

European Medicines Agency. Sales of veterinary antimicrobial agents in 31 European countries in 2017. European Surveillance of Veterinary Antimicrobial Consumption, 2019.

Gao Y. Q.; Gao N. Y.; Deng Y.; Gu J. S.; Gu Y. L.; Zhang D. Factor affecting sonolytic degradation of sulfamethazine in water. Ultrasonics Sonochemistry. 2013 Nov; 20(6): 1401-1407.

Gao Y. Q.; Gao N. Y.; Deng Y.; Yang Y. Q.; Ma Y. Ultraviolet (UV) light-activated persulfate oxidation of sulfamethazine in water. Chemical Engineering Journal. 2012 Jul; 95-196: 248-253.

Garcià-Galàn M. J., Diàz-Cruz M. S. and Barcelò D. Identification and determinationof metabolites and degradationproducts of sulfonamide antibiotics. Trends in Analytical Chemistr. 2008 Dec; 27(11): 1008-1022.

García-Galán M. J., Díaz-Cruz M. S. and Barceló D. Kinetic studies and characterization of photolytic products of sulfamethazine, sulfapyridine and their acetylated metabolites in water under simulated solar irradiation. Water Research. 2012 Mar; 46(3): 711-722.

Garoma T., Umamaheshwar S. K. and Mumper A. Removal of sulfadiazine, sulfamethizole, sulfamethoxazole, and sulfathiazolefrom aqueous solution by ozonation. Chemosphere. 2010 May; 79(8): 814–820.

Ge L.; Zhang P.; Halsall C.; Li Y.; Chenc C. E.; Li J.; Sun H.; Yao Z. The importance of reactive oxygen species on the aqueous phototransformation of sulfonamide antibiotics: kinetics, pathways, and comparisons with direct photolysis. Water Research. 2019 Feb; 149(1): 243-250.

Gome A. and Upadhyay K. Chemical Kinetics Of Ozonation and Other Processes Used for the Treatment of Wastewater Containing Pharmaceuticals; A Review. International Journal of Current Research and Review. 2012 Nov; 4(22): 157-168.

Gothwal R. and Shashidhar T. Antibiotic Pollution in the Environment: A Review. Clean - Soil, Air, Water. 2014 Jul; 42(9999): 1-11.

Graham J. P.; Evans S. L.; Prince L. B.; Silbergeld E. K. Fate of antimicrobial-resistant enterococci and staphylococci and resistance determinants in stored poultry litter. Environmental Research. 2009 Aug; 109(6): 682-689.

Gurol M. D. and Akata A. Kinetics of ozone photolysis in aqueous solution. Environmental and Energy Engineering. 1996 Nov; 42(11): 3283-3292.

Hatchard C. G. and Parker C. A. Potassium ferrioxalate as a standard chemical actinometer. 1956 Jun; 235(1203).

Henry R. J. The mode of action of Sulfonamides. Bacteriology Reviews. 1943 Dec; 7(4): 175-262.

Hernandez R.; Zappi M.; Colluci J.; Jones R. Comparing the performance of various advanced oxidation process for treatment of acetone contaminated water. Journal of Hazardous Materials. 2002 May; 92(1): 33-50.

Homem V. and Santos L. Degradation and removal methods of antibiotics from aqueous matrices - A review. Journal of Environmental Management. 2011 Oct; 92(10): 2304-2347.

Hou H.; Duan L.; Zhou B.; Tian Y.; Wei J.; Qian F. The performance and degradation mechanism of sulfamethazine from wastewater using IFAS-MBR. Chinese Chemical Letters. 2020; 31(02): 543–546.

Hou J.; Wan W.; Mao D.; Wang C.; Mu Q.; Qin S.; Luo Y. Occurrence and distribution of sulfonamides, tetracyclines, quinolones, macrolides, and nitrofurans in livestock manure and amended soils of Northern China. Environmental Science and Pollution Research. 2015 Mar; 22(6): 4545–4554.

Hu X. Zhou Q. and Luo Y. Occurrence and source analysis of typical veterinary antibiotics in manure, soil,vegetables and groundwater from organic vegetable bases, northern China. Environmental Pollution. 2010 Sep; 158(9): 2992-2998.

Iglesias A.; Nebot C.; Vázquez B. I.; Miranda J. M.; Abuín C. M. F.; Cepeda A. Detection of veterinary drug residues in surface waters collected nearby farming areas in Galicia, North of Spain. Environmental Science and Pollution Research. 2014 Feb; 21(3): 2367–2377.

Ikehata K., Naghashkar N. J. and El-Din M. G. Degradation of Aqueous Pharmaceuticals by Ozonation and Advanced Oxidation Processes: a Review. Ozone: Science and Engineering. 2006 Jun; 28(6): 353-414.

Indranil S. and Samiran B. Antimicrobial Resistance in Agriculture: Perspective, Policy and Mitigation. Elsevier - Academic Press, 2020.

Ji K.; Kim S.; Han S.; Seo J.; Lee S.; Park Y.; Choi K.; Kho Y. L.; Kim P. G.; Park J.; Choi K. Risk assessment of chlortetracycline, oxytetracycline, sulfamethazine, sulfathiazole, and erythromycin in aquatic environment: are the current environmental concentrations safe? Ecotoxicology. 2012 Oct; 21(7): 2013-2050.

Kaniou S.; Pitarakis K.; Barlagianni I.; Poulios I. Photocatalytic oxidation of sulfamethazine. Chemosphere. 2005 Jul; 60(3): 372-380.

Kim K. R.; Owens G.; Kwon S. I.; So K. H.; Lee D. B.; Ok Y. S. Occurrence and Environmental Fate of Veterinary Antibiotics in the Terrestrial Environment. Water, Air and Soil Pollution. 2011 Jan; 214(1-4): 163-174.

Kim Y.; Choi K.; Jung J. Y.; Park S.; Kim P.; Park J. Aquatic toxicity of acetaminophen, carbamazepine, cimetidine, diltiazem, and six major sulfonamides, and their potential ecological risks in Korea. Environment International. 2007 Apr; 33(3): 370–375.

Kirchhelle C. Pharming animals: a global history of antibiotics in food production (1935-2017). Palgrave Commununications. 2018 Aug; 4(96).

Kukui A., Roggenbuck J. and Schindler R. N. Mechanism and rate constants for the reactions of Cl atoms woth HOCl, CH_3OCl and tert-C_4H_9OCl. Berichte del Bunsengesellschaft fur physikalische Chemie. 1997 Feb; 101(2): 281-286.

Kümmerer K. Antibiotics in the aquatic environment – A review – Part I. Chemosphere. 2009 Apr; 75(4): 417-434.

László Zs. Investigation of applicability of VUV photolyis for degradation of organic pollutants. University of Szeged, 2001.

Lertpaitoonpan W. Sorption, degradation, and transport of sulfamethazine in soils and manure-amended soils. 2008. Graduate Theses and Dissertations. 11180.

Lertpaitoonpan W., Ong S. K. and Moorman T. B. Effect of organic carbon and pH on soil sorption of sulfamethazine. Chemosphere. 2009 Jul; 76(4): 558–564.

Li M.; Wang C.; Yau M.; Bolton J. R.; Qiang Z. Sulfamethazine degradation in water by the VUV/UV process: Kinetics, mechanism and antibacterial activity determination based on a mini-fluidic VUV/UV photoreaction system. Water Research. 2017 Jan; 108: 348-355.

Lin A. Y.; Lin C. F.; Chiou J. M.; Hong P. K. O_3 and O_3/H_2O_2 treatment of sulfonamide and macrolide antibiotics in wastewater. Journal of Hazardous Materials. 2009 Nov; 171(1-3): 452-458.

Liu N.; Huang W.-y.; Li Z.-m.; Shao H.-y.; Wu M.-h.; Lei J.-q.; Tang L. Radiolytic decomposition of sulfonamide antibiotics: Implications to the kinetics, mechanisms and toxicity. Separation and Purification Technology. 2018 Mar; 202: 259-265.

Martinez J. L.; Fajardo A.; Garmendia L.; Hernandez A.; Linares J.F.; Martínez-Solano L.; Sánchez M. B. A global view of antibiotic resistance. FEMS Microbiology Reviews. 2009 Jan; 33(1): 44-65.

Martınez-Carballo E.; Gonzalez-Barreiro C.; Scharf S.; Gans O. Environmental monitoring study of selected veterinary antibiotics inanimal manure and soils in Austria. Environmental Pollution. 2007 Jul; 148(2): 570-579.

McManus M.C. Mechanisms of bacterial resistance to antimibiobial agents. American Journal of Health-System Pharmacy. 1997 Jun; 54(12): 1420-1433.

Mora A. S. and Mohseni M. Temperature dependence of the absorbance of 185 nm photons by water and commonly occurring solutes and its influence on the VUV advanced oxidation process. Environmental Science: Water Research & Technology. 2018 Jun; 4(8).

Murov S.L. Handbook of Photochemistry. New York: Marcel Dekker, 1973.

Náfrádi M.; Farkas L.; Alapi T.; Hernádi K.; Kovács K.; Wojnárovits L.; Takács E. Application of coumarin and coumarin-3-carboxylic acid for the determination of hydroxyl radicals during different advanced oxidation processes. Radiation Physics and Chemistry. 2020 May; 170.

Nassar R.; Trivella, A.; Mokh, S.; Al-Iskandarani, M.; Budzinski, H.; Mazellier, P. Photodegradation of sulfamethazine, sulfamethoxypiridazine, amitriptyline, and clomipramine drugs in aqueous media. Journal of Photochemistry and Photobiology A: Chemistry. 2017 Mar; 336: 176-182.

Oppenländer T. Mercury-free sources of VUV/UV radiation: Application of modern excimer lamps (excilamps) for water and air treatment. Journal of Environmental Engineering and Science. 2007 May; 6(3): 253-264.

Oppenländer T.; Walddorfer C.; Burgbacher J.; Kiermeier M.; Lachner K.; Weinschrott H. Improved Vacuum-UV(VUV)-Initiated Photo-Mineralization of Organic Compounds in Water With Xenon Excimer Flow-Through photoreactor (Xe_2* lamp. 172 nm) Containing an Axially Centered Ceramic Oxygenator. Chemosphere. 2005 Jul; 60(3): 302-309.

Oppenländer T. Photochemical Purification of Water and Air. Darmstadt: WILEY-VCH, 2003.

Oturan A. M. and Aaron J. J. Advances Oxidation Processes in Water/Wastewater Treatment: Principles and Applications. A review. Critical Reviews in Environmental Science and Technology. 2014 Dec; 44(23): 2577-2641.

Parsons S. Advanced Oxidation Processes for Water and Wastewater treatment [Book]. - London : IWA Publishing, 2004.

Pérez-Moya M.; Graells M.; Castells G.; Amigò J.; Ortega E.; Buhigas G.; Pérez L. M.; Mansilla, H.D. Characterization of the degradation performance of the sulfamethazine antibiotic by photo-Fenton process. Water Research. 2010 Feb; 44(8): 2533-2540.

Price L. B.; Johnson E.; Vailes R.; Silbergerd E. Fluoroquinolone-resistant Campylobacter isolates from conventional and antibiotic-free chicken products. Environmental Health Perpectives. 2005 May, 113(5): 557-560.

Ragnar M., Eriksson T. and Reitberger T. Radical Formation in Ozone Reactions with Lignin and Carbohydrate Model Compounds. Holzforschung. 1999 Jan; 53(3): 292-298.

Reybroeck W.; Jacobs F. J.; De-Brabander H. F.; Daeseleire E. Transfer of Sulfamethazine from Contaminated Beeswax to Honey. Journal of Agricultural and Food Chemistry. 2010 May; 58(12): 7258–7265.

Rodrìguez-Chueca J.; Amor C.; Silvia T.; Dionysiou D.; Puma G. L.; Lucas M. S.; Peres J. A. Treatment of winery wastewater by sulphate radicals: HSO_5^-/transition metal/UV-A LEDs. Chemical Engineering Journal. 2016 Apr; 310.

Rodriguez-Narvaez O.; Peralta-Hernandez J. M.; Goonetilleke A.; Bandala E. R. Treatment technologies for emerging contaminants in water: A review. Chemical Engineering Journal. 2017 Apr; 323(1): 361-380.

Sági G.; Csay T.; Szabó L.; Pátzay G.; Csonka E.; Takács E.; Wojnárovits L. Analytical approaches to the OH radical induced degradation of sulfonamide antibiotics in dilute aqueous solutions. Journal of Pharmaceutical and Biomedical Analysis. 2015 Mar; 106: 52-60.

Schug K. A. Pseudo-molecular Ion Formation by Aromatic Acids in Negative Mode Electrospray Ionization Mass Spectrometry. Blacksburg, Virginia: Department of Chemistry , 2002 Oct.

Silverman R. B. The Organic Chemistry of Drug Design and Drug Action. San Diego: CA Academic Press, 1992.

Smith T. C.; Gebreyes W. A.; Abley M. J.; Harper A. L.; Forshey B. M.; Male M. J.; Martin H. W.; Molla B. Z.; Sreevatsan S.; Thakur S.; Thiruvengadam M.; Davies P. R. Methicillin-resistant Staphylococcus aureus in pigs and farm workers on conventional and antibiotic-free swine farms in the USA. PLoS ONE. 2013 May; 8(5): e63704.

Šojić D.; Despotović V.; Orčić D.; Szabó E.; Arany E.; Armaković S.; Illés E.; Gajda-Schrantz K.; Dombi A.; Alapi T.; Sajben-Nagy E.; Palágyi A.; Vágvölgyi C.; Manczinger L.; Bjelica L.; Abramović B. Degradation of thiamethoxam and metoprolol by UV, O_3 and UV/O_3 hybrid processes: Kinetics, degradation intermediates and toxicity. Journal of Hydrology. 2012 Nov; 472-473: 314-327.

Sukul P. and Spiteller M. Sulfonamides in the Environment as Veterinary Drugs. In: Reviews of Environmental Contamination and Toxicology. New York: Springer, 2006; 187: 67-101.

Svestkova T.; Macsek T.; Landova P.; Utersky M.; Vavrova M.; Hlavinek P. Use of Advanced Oxidation Processes for Water Treatment. Fresenius Environmental Bulletin. 2019; 28(2): 831-836.

Solarchem Environmental Systems. The UV/oxidation handbook. Markham, Ont., Canada; Las Vegas, Nev.: Solarchem Environmental Systems. 1994.

Tačić A.; Nikolić V.; Nikolić L.; Savić I. Antimicrobial Sulfonamide Drugs. Advanced Technologies. 2017 May; 6(1): 58-71.

Takács-Novák K., Józan M. and Szász G. Lipophilicity of amphoteric molecules expressed by the true partition coefficient. International Journal of Pharmaceutics. 1995 Jan; 113(1): 47-55.

The Council of The European Union. Ed. 96/23/EC Council Directive. Official Journal, 1996; 125: 10-32.

Thiele-Bruhn S. Pharmaceutical Antibiotic Compounds in Soils – A Review. Journal of Plant Nutrition and Soil Science. 2003 Aug; 166(2): 145-167.

Thomsen C. L.; Madsen D.; Keiding S. R.; Thøgersen J.; Christiansen O. Two-photon dissociation and ionization of liquid water studied by femtosecond transient absorption spectroscopy.The Journal of Chemical Physics. 1999 Feb; 110(3453).

Tolls J. Sorption of veterinary pharmaceuticals in soils: a review. Environmental Science and Technology. 2001 Sep; 35(17): 3397-3406.

Van Boeckel T. P.; Brower C.; Gilbert M.; GrenfelL B. T.; Levin S. A.; Robinson T. P.; Teillant A.; Laxminarayan R. Global trends in antimicrobial use in food animals. Proceedings of the National Academy of Sciences of the Unite States of America. 2015 May; 112(18): 5649-5654.

von Sonntag C and von Guten U. Chemistry of Ozone in Water and Wastewater Treatment. From Basic Principles to Applications. London: IWA Publishing, 2012.

Wang D., Bolton J. R. and Hofmann R. Medium pressure UV combined with chlorine advanced oxidation for trichloroethylene destruction in a model water. Water Research. 2012 Oct; 46(15): 4677-4686.

Wegst-Uhrich S. R.; Navarro D. A. G.; Zimmerman L.; Aga D. S. Assessing antibiotic sorption in soil: a literature review and new case studies on sulfonamides and macrolides. Chemistry Central Journal. 2014 Jan; 8(1): 5.

Wei R.; Ge F.; Huang S.; Chen M.; Wang R. Occurrence of veterinary antibiotics in animal wastewater and surface wateraround farms in Jiangsu Province, China. Chemosphere. 2011Mar; 82(10): 1408-1414.

The merck index, 10th Ed. Edited By Martha Windholz. USA: Merck & Co., 1983.

Wojnárovits L., Tóth T. and Takács E. Critical evaluation of rate coefficients for hydroxyl radical reactions with antibiotics: A review. Critical Reviews in Environmental Science and Tecnology. 2018 Jul; 48(6): 575-613.

Xiang H.; Shao Y.; Gao N.; Lu X.; Chu W.; An N.; Tan C.; Zheng X.; Gao Y. The influence of bromide on the degradation of sulfonamides in UV/free chlorine treatment: Degradation mechanism, DBPs formation and toxicity assessment. Chemical Engineering Journal. 2019 Jan; 362: 692-701.

Yao L.; Wang Y.; Tong L.; Li Y.; Deng Y.; Guo W.; Gan Y. Seasonal variation of antibiotics concentration in the aquatic environment: a case study at Jianghan Plain, central China. Science of The Total Environment. 2015 Sep; 527-528: 56-64.

Yi Z.; Wang J.; Tang Q.; Jiang T. Photolysis of sulfamethazine using UV radiation in an aqueous medium.The Royal Society of Chemistry. 2018 Jan; 8(3): 1427-1435.

Zeng E. Y. Persistent Organic Pollutants (POPs): Analytical Techniques, Environmental Fate and Biological Effects. Amsterdam: Elsevier, 2015.

Zhang R.; Yang Y.; Huang. C. H.; Zhao L.; Sun P. Kinetics and modeling of sulfonamide antibiotic degradation inwastewater and human urine by UV/H_2O_2 and UV/PDS. Water Research. 2016 Oct; 103: 283-292.

Zhu G.; Sun Q.; Wang C.; Yang Z.; Xue Q. Removal of Sulfamethoxazole, Sulfathiazole and Sulfamethazine in their Mixed Solution by UV/H_2O_2 Process. International Journal of Environmental Research and Public Health. 2019 May; 16(10): 1797

AZoOptics. Applications of Ultra-Violet LEDs and Safety Considerations. Optoelectronics Marktech. 2016. Date of access: 03 05 2020.
- https://www.azooptics.com/Article.aspx?ArticleID=1087.

EPA DSSTox Database. Date of access: 08 05 2020.
-https://www.epa.gov/chemical-research/distributed-structure-searchable-toxicity-dsstox-database.

Estimation Program Interface (EPI). EPA US. 2012. Date of access: 08 05 2020.
-http://www2.epa.gov/tsca-screening-tools.

Veterinary Substances DataBase (VSDB). Hertfordshire University. Date of access: 08 05 2020.
-https://sitem.herts.ac.uk/aeru/vsdb/Reports/1829.htm.

SPW Industrial. Date of access: 16 05 2020.

-https://spwindustrial.com/agilent-hp-8453-uv-visible-spectrophotometer-g1103a-with-computer-chem-sw/.

Universiity of Bologna - Department of Chemistry "Giacomo Ciamician". Date of access: 16 05 2020.
-https://chimica.unibo.it/it/ricerca/laboratori-di-ricerca/laboratorio-analisi-strumentali-chimica-organica.

Trident Processes. Date of access: 03 05 2020.
- https://tridentprocesses.com/solutions/wastewater-treatment/.

Microbewiki. Date of access: 03 06 2020.
- https://microbewiki.kenyon.edu/index.php/Vibrio_fischeri

Kunkel Dennis. Vibro fischeri image. Microscopy/science Photo Library. 15 09 2018. Date of access: 11 05 2020.
-https://fineartamerica.com/featured/vibrio-fischeri-dennis-kunke-microscopyscience-photo-library.html.